Evolution of arc-continent collision in the southeastern margin of the South China Sea: Insight from the Isugod Basin in central-southern Palawan

Wen-Huang Chen[1, 2, 3], Yi Yan[1, 2, 3*], Andrew Carter[4], Peter D. Clift[5, 6], Chi-Yue Huang[7], Graciano P. Yumul Jr.[8], Carla B. Dimalanta[9], Jillian Aira S. Gabo-Ratio[9], Le Zhang[1], Ming-Huei Wang[10], Xin-Chang Zhang[1]

[1]State Key Laboratory of Isotope Geochemistry, Guangzhou Institute of Geochemistry, Chinese Academy of Sciences, Guangzhou 510640, China

[2]CAS Center for Excellence in Deep Earth Science, Guangzhou 510640, China

[3]Key Laboratory of Ocean and Marginal Sea Geology, Guangzhou Institute of Geochemistry, Chinese Academy of Sciences, Guangzhou 510640, China

[4]Department of Earth and Planetary Sciences, Birkbeck, University of London, Malet Street, London, WC1E 7HX, United Kingdom

[5]Department of Earth Sciences, University College London, London WC1E 6BS, United Kingdom

[6]Department of Geology and Geophysics, Louisiana State University, Baton Rouge, LA, USA

[7]School of Ocean and Earth Science, Tongji University, Shanghai 200092, China

[8]Cordillera Exploration Company Incorporated, NAC Tower, Bonifacio Global City, Taguig, Metro Manila 1634, Philippines

[9]Rushurgent Working Group–Tectonics and Geodynamics Academic Group, National Institute of Geological Sciences, College of Science, University of the Philippines Diliman, Quezon City 1101, Philippines

[10]Exploration and Development Research Institute, CPC Corporation, Taiwan, Miaoli 36042, Taiwan

*Corresponding Authors: Yi Yan yanyi@gig.ac.cn

Key Points:

- Sediments in the Isugod Basin were deposited at 11.5–5.6 Ma following local gravitational collapse of the Palawan wedge driven by uplift
- The Isugod Basin sediments were supplied by erosion of the Palawan wedge and obducted forearc ophiolite exposed subaerially since ~11.5 Ma
- Onset of Palawan arc-continent collision at ~18 Ma followed by a significant uplift pulse in the Palawan wedge beginning within 13.4–11.5 Ma

Abstract

The evolution of arc-continent collision between the Palawan microcontinental block and the Cagayan Ridge in the southeastern margin of the South China Sea (SCS) is vital to understand how this collision correlated with seafloor spreading of the SCS. To address the evolution of arc-continent collision, we studied the biostratigraphy and provenance of syn-collisional sediments in the Isugod Basin in central-southern Palawan. Microfossil analysis indicates a Late Miocene age (11.5–5.6 Ma) for the Isugod and Alfonso XIII Formations and rapid subsidence during initiation of the basin which may have been triggered by local extensional collapse of the wedge in response to forearc uplift. Multidisciplinary provenance analysis reveals that the Isugod and Alfonso XIII Formations were derived from the Middle Eocene–lower Oligocene Panas-Pandian Formation on the Palawan wedge and the Late Eocene Central Palawan Ophiolite. These results suggest the emergence of both the orogenic wedge and obducted forearc ophiolite at ~11.5 Ma, implying collision onset before ~11.5 Ma. The collision initiation in Palawan could be better constrained to ~18 Ma, based on the drowning of the Nido carbonate platform in the foreland. Therefore, the gravitational collapse of the Palawan wedge and the subsidence/formation of the Isugod Basin might reflect a significant uplift pulse in the hinterland of the wedge beginning within 13.4–11.5 Ma in the late stage of collision. It indicates that although compression originated from spreading of the SCS had ceased at 16–15 Ma, arc-continent collision in Palawan did not stop and was sustained by compression from the upper plate afterwards.

Plain Language Summary

The Palawan microcontinental block is a continental fragment separated from the South China margin along with the seafloor spreading of the South China Sea (SCS). It finally collided with the Cagayan Ridge volcanic arc because of southward subduction of the Proto-SCS. Therefore, precisely constraining the evolution of arc-continent collision could help us to understand its association with the ending of the SCS spreading. To constrain the evolution of arc-continent collision, we determined the depositional age and source of syn-collisional sediments in the Isugod Basin in central-southern Palawan. Our results shows that the Isugod Basin sediments were deposited during the Late Miocene (11.5–5.6 Ma) following local gravitational collapse of the Palawan orogenic wedge driven by uplift and oversteepening. Isugod Basin sediments were eroded from both the orogenic wedge and obducted forearc ophiolite that were uplifted and exposed subaerially, indicating collision began before ~11.5 Ma. As the onset of collision could be constrained to ~18 Ma, we propose a significant uplift pulse in the hinterland of the wedge began at 13.4–11.5 Ma in the late stage of collision. This further indicates that arc-continent collision in Palawan did not stop although compression derived from spreading of the SCS had ceased at 16–15 Ma.

1. Introduction

Arc-continent collision is one of the fundamental tectonic processes driving the growth of continental crust (e.g. Clift et al., 2003; Rudnick et al., 1995). At the same time obduction of forearc or protoarc oceanic lithosphere (ophiolite) onto continents may further play a major role in climate change, especially when the arc-continent collision occurs in the tropics (Macdonald, 2019; Jagoutz et al., 2016). Southeast Asia and adjoining regions comprise a complex collages of continental terranes, volcanic arcs, and remnants of oceanic basins. The area provides typical examples of modern arc-continent collision, such as Taiwan, Timor and New Guinea (e.g. Abbot, 1994; Harris, 2011; Huang et al., 2006). Relatively, little has been known about the arc-continent collision along the southeastern margin of the South China Sea (SCS) (e.g. Keenan et al., 2016; Rangin & Silver, 1991).

Since initiation of seafloor spreading in the SCS during the Early Oligocene (~33 Ma), the Palawan microcontinental block and the Dangerous Grounds (Figure 1a) drifted away from the South China margin, accommodated by southward subduction of the Proto-SCS beneath northern Borneo and the Cagayan Ridge volcanic arc (e.g. Holloway, 1982; Taylor & Hayes, 1983). Therefore, precisely constraining the evolution of the collision between the microcontinental blocks and the northern Borneo and the Cagayan Ridge volcanic arc would be vital to understand how this collision correlated with the seafloor spreading of the SCS, especially the cessation of the seafloor spreading at 16–15 Ma (Briais et al., 1993; Li et al., 2014). Collision of the Dangerous Grounds along the southwestern margin of the SCS with the active continental margin of Sabah in northern Borneo (Figure 1a) is commonly thought to have commenced in the Early Miocene, marked by the regional Top Crocker Unconformity (=Base Miocene Unconformity) (Hall, 2013; van Hattum et al., 2013). A recent reexamination on this unconformity (Lunt, 2022) suggested that it could be placed at ~23 Ma. However, east of Sabah, the timing of initial collision between the Palawan microcontinental block and the Cagayan Ridge volcanic arc is more controversial. This calls into question whether arc-continent collision in Palawan was diachronous or synchronous with collision in northern Borneo. Rangin & Silver (1991) proposed ~16 Ma for cessation of the volcanism along the Cagayan Ridge, attributed to initiation of the arc-continent collision. By dating two carbonate sequences above and below the offshore Palawan wedge (the Nido Limestone and the Tabon Limestone, respectively), Steuer et al. (2013) suggested that arc-continent collision in Palawan did not start before ~18 Ma and might have continued until ~7 Ma. Obduction of forearc ophiolite onto the continental margin has been observed in most arc-continent collisions, especially those involving Tethyan or northern Australian margins (Harris, 2011; Rolland et al., 2020). This process also occurred in Palawan and was regarded as typical of arc-continent collision (e.g. Keenan et al., 2016). Hall (2013) proposed that the Palawan microcontinental block began to collide with the Cagayan Ridge in the Early Miocene (~20 Ma), almost coeval with the collision in northern Borneo. This model is supported by evidence from the Lower Miocene Tajau Sandstone Member in northernmost Sabah that was sourced from the metamorphic sole of the obducted Palawan Ophiolite. However, a recent biostratigraphic study of the Tajau Sandstone Member suggested a depositional age during the Late Oligocene–Early Miocene (Lunt & Madon, 2017) or Early-Middle Eocene (Rahim et al., 2017), making it doubtful that the Tajau Sandstone Member recorded the arc-continent collision in Palawan. As to the evolution of arc-continent collision in Palawan, it is notable that gravity-driven processes (linked listric normal fault–toe thrust systems and mass transport complexes) occurred in the most external part of the Palawan wedge (Ilao et al., 2018). These processes were inferred to respond to collisional thickening-related uplift (Ilao et al., 2018). However, it remains largely unknown how these processes linked to the tectonics onland Palawan.

In central-southern Palawan, thrust faulting related to obduction of the ophiolite was sealed by Neogene sedimentary rocks of the Isugod Basin (the Isugod and Alfonso XIII Formations) (Aurelio et al., 2014). The formation of the basin was assumed to be controlled by normal faulting although no normal faults bounding the basin were directly observed from the field (Aurelio et al., 2014). Preliminary provenance analysis indicated that the source of sediment to the Isugod Formation included both the Palawan Ophiolite and the Palawan microcontinental block (Suggate et al., 2014). These observations suggest that Isugod Basin sediments may be vital to understand the arc-continent collision in Palawan. Although the depositional age of the Isugod Formation has not been well constrained, Suggate et al. (2014) arbitrarily assigned it to the Lower Miocene equivalent to the Tajau Sandstone Member in northernmost Sabah. To better constrain the evolution of collision between the Palawan microcontinental block and the Cagayan Ridge, we conducted a detailed biostratigraphic and provenance study of Isugod Basin sediments. Specifically, we determined depositional ages using integrated biostratigraphy based on both planktonic foraminifera and calcareous nannofossils. Benthic foraminifera were also used to reveal the variations in the depositional environment in response to collision. As the potential source areas, the Palawan microcontinental block and the Palawan Ophiolite have contrasting lithologies and geochemistry, we adopted a multidisciplinary approach using trace elements, Nd isotopes, heavy mineral assemblages as well as detrital zircon U-Pb geochronology to trace sediment provenance for the entire Isugod Basin.

2. Geologic Setting

2.1. Geology offshore Palawan

The Palawan microcontinental block spans the area of Palawan, Mindoro, western Panay, the Romblon Islands and Reed Bank (Figure 1a) (Hinz & Schlüter, 1985; Holloway, 1982; Liu et al., 2014; Yumul et al., 2009). The northeast-southwest oriented islands of Palawan lie on the southeastern margin of the block. The Palawan Trough to the northwest of central-southern Palawan (Figures 1a and 1d) was interpreted as a flexural foreland depression formed because of loading by the northwestward emplacement of the Palawan wedge onto the thinned Palawan microcontinental crust when the microcontinent collided with the Cagayan Ridge (Hinz & Schlüter, 1985; Rangin & Silver, 1991). The Palawan wedge (= Pulute wedge of Steuer et al., 2013 or Pagasa wedge of Aurelio et al., 2014) is an deep-water orogenic wedge composed mainly of deformed and imbricated continental slope sedimentary rocks involved in the arc-continent collision (Rangin & Silver, 1991), including the Eocene–Lower Oligocene Pulute Formation and the Lower–Middle Miocene Pagasa Formation that displays fold and thrust structures (Aurelio et al., 2014) (Figure 1d). Although an accretionary wedge would not be expected to develop in an intra-oceanic subduction setting, accretion could occur as the arc begins to collide with a passive continental margin and these sediment were accreted (Draut & Clift, 2012). In this sense, the Palawan wedge represents an orogenic wedge (e.g. Morley, 2024) rather than a classic accretionary wedge that generates during the subduction of the oceanic crust in the lower plate. The wedge was developed by a combination of crustal shortening and gravitational collapse (Morley et al, 2023). Underthrusting of a carbonate platform (the Upper Oligocene–Lower Miocene Nido Limestone widespread in the Palawan Trough and on the northwestern Palawan shelf) beneath the external part of the wedge was widely observed from the seismic profile offshore southwest Palawan (Steuer et al., 2013, Aurelio et al. 2014). The top of the resistant Nido Limestone might acts as a décollement/detachment surface (Steuer et al., 2013, Ilao et al., 2018), above which the younger and less resistant shale-prone unit (the Pagasa Formation) was added into the orogenic wedge through frontal accretion. However, deeper into the thrust fold zone, wedge-related thrusting also involved scrapping off of the Nido Limestone and even the deeper Eocene clastics of the Pulute Formation underlying the Nido Limestone (Aurelio et al., 2014; Ilao et al., 2018; Morley et al., 2023). This might indicate the upward propagation of the décollement from deeper stratigraphic layer to the top of the Nido Limestone/base of the Pagasa Formation. Gravity-driven processes that include linked listric normal fault–toe thrust systems, mass transport complexes are reported from the most external part of the Palawan wedge, where the Pagasa Formation is dominated (Ilao et al., 2018).

The submerged Cagayan Ridge (Figure 1a) represents the extinct volcanic arc associated with subduction of the Proto-SCS beneath the Sulu Sea (Holloway, 1982; Rangin & Silver, 1991). The Cagayan Ridge divided the Sulu Sea into the NW Sulu Sea forearc basin and the SE Sulu Sea backarc basin (Liu et al., 2014; Rangin & Silver, 1991). Gravity and magnetic studies suggested that the NW Sulu Sea was mainly floored by a relict Late Createaceous to Eocene oceanic slice (Liu et al., 2014). However, a recent seismic interpretation revealed rift-related depocenters overlying crystalline basement in the southeastern part of the NW Sulu Sea, and the rift-related depocenters consists of uncalibrated but tentatively dated Paleogene to Lower Miocene units (Cadenas & Ranero, 2024). The Cagayan Ridge runs approximately parallel to Palawan Island, and extends northward to the islands of Panay, Romblon and Mindoro (Bellon & Rangin, 1991; Marchadier & Rangin, 1990) (Figure 1a). The Cagayan Ridge also extends westwards to Sandakan in Sabah where an un-reset apatite fission-track age of 33.9±7.7 Ma represents the oldest available age for arc volcanism (Hutchison et al., 2000). An age of ~16 Ma, constrained by paleomagnetism and radiolarian biostratigraphy, for the top of pyroclastic sediments recovered at Ocean Drilling Program (ODP) Site 768 in the SE Sulu Sea basin (distal to the Cagayan Ridge) provides a timing for cessation of arc volcanism (Rangin & Silver, 1991). However, the top of volcaniclastic sedimentary rocks at ODP Site 771 on the southeastern flank of the Cagayan Ridge was dated at Zone NN5 (13.5–14.9 Ma) (Rangin & Silver, 1991). Andesite samples dredged from the crest of the ridge yielded a K-Ar age as young as 10.7±1.5 Ma (Kudrass et al., 1990).

2.2. Geology Onshore Palawan

Along the Ulugan Bay Fault, Palawan is divided into two tectonic domains; northern and central-southern Palawan (Wolfart et al., 1986) (Figure 1b). Northern Palawan is subdivided into the Malampaya Sound Group and the Barton Group. The Malampaya Sound Group is a succession of chert, siliciclastic sedimentary rocks and carbonate spanning from the Upper Paleozoic to the Mesozoic (Aurelio & Peña, 2010). The Barton Group is composed of a very low to low grade metamorphosed Upper Cretaceous sedimentary succession that was deposited along the South China margin (e.g. Walia et al., 2012). The Barton Group is subdivided into three units, and these units were considered to be continuous and are stratigraphically arranged from bottom to top as follows: the Caramay Schist, the Concepcion Phyllite and the Boayan Formation (Aurelio & Peña, 2010; Suzuki et al. 2000).

Central-southern Palawan is assumed to be the emergent Palawan wedge overthrust northwestward by ophiolite nappes subsequent to the Miocene collision (Hinz & Schlüter, 1985) (Figure 1b). The Palawan Ophiolite are subdivided into the Late Eocene Central Palawan Ophiolite and the Cretaceous Southern Palawan Ophiolite (e.g. Dycoco et al., 2021; Keenan et al., 2016). The Central Palawan Ophiolite is the dominant ophiolite unit in Palawan. It forms the onland extension of the NW Sulu Sea and represents fragments of a Late Eocene oceanic basin within an initially Cretaceous Proto-SCS, where the active spreading center rapidly converted to a south-dipping subduction zone at ~34 Ma (Keenan et al., 2016). The metamorphic sole of the Central Palawan Ophiolite and comprises high-grade metamorphic rocks (such as kyanite-garnet amphibolites, epidote amphibolites and kyanite schists) and is exposed at Dalrymple Point (Figure 1b) along Ulugan Bay (Keenan et al., 2016). Thermobarometric studies on the metamorphic sole show that it developed during initiation of Eocene subduction (Encarnación et al., 1995; Valera et al., 2021). This process was called detachment of the ophiolite by Encarnación et al. (1995). Although some researchers also defined the inception of subduction and consequent development of a metamorphic sole beneath an ophiolite as obduction (emplacement), or at least first stage of obduction (Wakabayashi and Dilek, 2003), in the context of this paper, the obduction of the Palawan Ophiolite refers its obduction onto the continental margin in response to arc-continent collision. A much smaller ophiolite in Southern Palawan (Southern Palawan Ophiolite) might represent remnants of the Cretaceous Proto-SCS oceanic lithosphere (Dycoco, et al., 2021). Both the Cretaceous and Eocene ophiolites were emplaced northwestward onto the Middle Eocene–lowermost Oligocene Panas-Pandian Formation during Miocene collision. The Panas-Pandian Formation represents non-metamorphosed syn-rift sedimentary rocks deposited prior to the onset of seafloor spreading of the SCS in the earliest Oligocene (e.g., Chen et al., 2021). These syn-rift sedimentary rocks exposed on land are the equivalent of the offshore Pulute Formation. The poorly exposed Ransang Limestone of Early Miocene age is correlative to the post-rift Nido Limestone that is widespread offshore Palawan and the St. Paul Limestone north of the Ulugan Bay Fault (Aurelio & Peña, 2010). A small outcrop of the Eocene Central Palawan Ophiolite has also been thrust over the metamorphosed Upper Cretaceous Barton Group north of the Ulugan Bay Fault (Figure 1b). Northern Palawan has experienced a greater level of exhumation of the ophiolite and sedimentary-metasedimentary rocks compared to central-southern Palawan (Keenan, 2016; Ilao et al., 2018). The Barton Group was assumed to be exhumed from the core of the Palawan wedge (Keenan, 2016), whereas the Panas-Pandian Formation might represent the sedimentary cover of the wedge. The thrust contact between the Central Palawan Ophiolite and the Panas-Pandian Formation was inferred to be sealed in the Isugod Basin by Miocene collision-related clastic and carbonate rocks (the Isugod Formation and Alfonso XIII Formation) (Aurelio et al., 2014) (Figure 1d). Detailed bedding measurements taken from the Alfonso XIII Formation (Rehm, 2002) document a NNE-SSW synclinal structure. A southwest-dipping normal fault, which postdates deposition of the Alfonso XIII Formation and caused the unit to be tilted, was inferred between the Alfonso XIII Formation and the Panas-Pandian Formation (Figure 1c) (Aurelio et al., 2014).

3. Materials and Methods

A suite of samples were collected from the Isugod and Alfonso XIII Formations for micropaleontology, trace element, Nd isotope and heavy mineral analyses as well as detrital zircon U-Pb geochronology. Specifically, eighteen mudstone samples and two limestone samples were collected from the Isugod Formation for species identification of planktonic and benthic foraminifera, together with calcareous nannofossils. Previously published data of trace element, heavy mineral and detrital zircons U-Pb age of the Isugod Formation (Cao et al., 2021; Suggate et al., 2014) were obtained from limited sampling near Site QU-26 in this study (Figure 1c). To complement these data we selected six mudstone samples for trace element and Nd isotopic analyses, four sandstone samples for heavy mineral analysis and detrital zircon U-Pb dating. Although 115 detrital zircon U-Pb ages from our samples QU-26a and QU-27a have been published collectively as Sample QU-26 in Yan et al. (2018), in this paper we report 157 new detrital zircon ages from these two samples and 214 detrital zircon ages from two new samples (QU-22a and QU-29a). We also collected four calcareous mudstone and one limestone sample from the Alfonso XIII Formation for microfossil analysis, of which three calcareous mudstone samples were chosen for trace element and Nd isotopic analyses. Full analytical methods are provided in Text S1 in the Supporting Information.

4. Results

4.1. Field Occurrence

The Isugod Formation is mainly distributed along the western flank of the Central Palawan Ophiolite in an NNE-SSW trending belt (Figure 1c). It consists of a rhythmic sequence of well-bedded sandstones and mudstones with limestone at the base. The strata generally dip 4°–22° towards the west, although local folds are common. The basal limestone is only ~20 m-thick, greyish white, hard and coralline and well-exposed at the Taraw Cave (Sites QU-02 and QU-03) (Figure 2a). The rhythmic sequence of sandstone and mudstone is ~800 m-thick and mainly observed along the Quezon-Aramaywan and Quezon-Aboabo roads (e.g. Site QU-12, Figure 2b). The sandstone is light grey, very thinly to thickly bedded and weakly consolidated, and the mudstone is dark grey, thinly to medium bedded (e.g., Sites QU-26 and QU-22, Figure 2c to 2e). Parallel and cross laminations are well developed in the sandstone, which shows other typical turbidite features (Bouma, 1962) (Figure 2d). Pebbly mudstones are occasionally observed at Site QU-13 in the lower part of the sequence. These are composed of rounded to subrounded, pebble- to cobble-sized clasts of volcanic rock, sandstone, mudstone and limestone suspended within a massive mudstone matrix. Coal lenses and amber were also reported in the pebbly mudstones (Aurelio & Peña, 2010). The pebbly mudstones are typical products of gravitational slumping or debris flow (Lowe, 1979). The Alfonso XIII Formation unconformably overlies the Isugod Formation and is mainly composed of well-consolidated, light grey to cream, thin- to thick-bedded limestones (Figure 2g) bearing coral and gastropod fossils. Well-bedded calcareous siltstone and mudstone are occasionally observed at sites QU-10, QU-16, QU-24 and QU-25 (Figures 2h and 2i).

4.2. Biostratigraphic Results

4.2.1. Planktonic foraminifera and calcareous nannofossils

Identified planktonic foraminifera and calcareous nannofossils are detailed in Supplementary Tables S1 and S2 and shown in Figure 3. Standard zonations of planktonic foraminifera established from low-latitude regions by Blow (1969) and datum planes (FAD: first appearance datum; LAD: last appearance datum) calibrated by Wade et al. (2011) were followed (Figure 4). The zonal scheme of calcareous nannofossils proposed by Martini (1971) and datum planes compiled by Anthonissen & Ogg (2012) were followed. An overall description of the microfossils is presented in Text S2, so that here we are strongly biased toward age-diagnostic fossils. Mudstone samples QU-13a and QU-26b in the siliciclastic succession of the Isugod Formation contain planktonic foraminifera of *Globigerina nepenthes* (FAD at 11.63 Ma), *Globigerina decoraperta* (FAD at 11.49 Ma) and *Globorotalia mayeri* (LAD at 10.46 Ma) and calcareous nannofossils of *Discoaster kugleri*, *Cocoolithus miopelagicus* (LAD at 10.97 Ma) and *Reticulofenestra pseudoumbilica* (FAD at 12.83 Ma). Although the FAD and LAD of common *Discoaster kugleri* at 11.90 Ma and 11.58 Ma, respectively, is a little older than the FAD of *Globigerina decoraperta* (11.49 Ma) (Figure 4), they are not in conflict because of the very low abundance of *Discoaster kugleri*. Therefore, samples QU-13a and QU-26b are assigned to Zone N14 or Zone NN7 (11.49–10.97 Ma) based on the concurrent occurrence of *Globigerina decoraperta* and *Cocoolithus miopelagicus* (Figure 4). The co-existence of *Globorotalia mayeri* (LAD at 10.46 Ma), *Discoaster hamatus* (FAD at 10.55 Ma; LAD at 9.53 Ma) and *Discoaster bollii* (LAD at 9.21 Ma) in Sample QU-12b indicates a depositional age near the boundary of Zones N14/N15 or Zones NN8/NN9 (10.55–10.46 Ma) (Figure 4). Sample QU-22b in the upper part of the Isugod Formation contains *Neogloboquadrina acostaensis* (FAD at 9.83 Ma) and *Discoaster hamatus* (FAD at 10.55 Ma; LAD at 9.53 Ma) but lacks of *Globorotalia mayeri* (LAD at 10.46 Ma), constraining this sample to being within Zone N16 or Zone NN9 (9.83–9.53 Ma)

(Figure 4). Based on the analyzed samples, the Isugod Formation can therefore be assigned to Zones N14–N16 or Zones NN7–NN9 (11.5–9.5 Ma) (Figure 4).

Within the younger Alfonso XIII Formation, *Neogloboquadrina acostaensis* (FAD at 9.83Ma) and *Globigerinoides extremus* (FAD at 8.93 Ma) commonly appear in calcareous mudstone samples QU-10c, QU-16c, QU-24 and QU-25. There are even younger species of *Globorotalia plesiotumida* (FAD at 8.58 Ma), *Globigerinoides conglobatus* (FAD at 6.20 Ma) and *Globorotalia margaritae* (FAD at 6.08 Ma) in Sample QU-25. However, Pliocene index species of *Globorotalia tumida* (FAD at 5.57 Ma) and *Sphaeroidinella dehiscens* (FAD at 5.53 Ma) has not been observed. Therefore, we assigned the Alfonso XIII Formation to Zones N16–N17B (8.93–5.57 Ma) (Figure 4). Calcareous nannofossils in the Alfonso XIII Formation, including *Discoaster hamatus* (FAD at 10.55 Ma; LAD at 9.53 Ma) and *Discoaster belleus* (FAD at 10.40 Ma) are likely of reworked origin. However, the appearance of *Discoaster asymmetricus* (Zones NN10–NN17) is consistent with the age determined from the planktonic foraminifera.

4.2.2. Benthic foraminifera

Benthic foraminifera from the Isugod and Alfonso XIII Formations are listed in Table S3 and shown in Figure S1. Rare specimens of benthic foraminifera, including larger foraminifera of *Amphistegina* spp. and small foraminifera of *Elphidium* spp. were obtained from the basal limestone of the Isugod Formation (Sample QU-02), indicating reef and forereef settings with water depths less than 50 m (BouDagher-Fadel, 2018; Murray, 1991) (Figure 5). Larger foraminifera of *Lepidocyclina* (*Nephrolepidina*) spp. spanning the Late Oligocene to Late Miocene in the Indo-Pacific (BouDagher-Fadel, 2018) were occasionally observed in thin section (Figure S2), roughly consistent with the Late Miocene age determined from the siliciclastic mudstones of the Isugod Formation. Diverse and abundant small benthic foraminifera were recovered from the siliciclastic mudstones (mainly in samples QU-12b and QU-13a). They are dominated by taxa with calcareous hyaline tests, such as *Uvigerina proboscidea*, *Uvigerina peregrina*, *Bulimina striata*, *Globocassidulina subglobosa*, *Pullenia bulloides*, *Melonis pompilioides*, *Gyroidinoides soldanii*, *Bolivinita quadrilatera*, *Oridorsalis umbonatus*, *Cibicidoides mundulus* and *Oolina hexagona*, suggesting a middle bathyal depth (600–1000 m) (Holbourn et al., 2013) of deposition (Figure 5).

Abundant larger and small benthic foraminifera were observed in the weakly consolidated limestone and calcareous mudstone (samples QU-01, QU-10c, QU-16c) of the Alfonso XIII Formation. The larger foraminifera are overwhelmed by *Amphistegin*a spp. and *Operculina* spp. and the small foraminifera are characterized by the occurrence of *Elphidium* spp., *Ammonia* spp., *Discorbis* spp., *Buccella* sp. and *Heterolepa* spp., which denotes reef and forereef environments (Figure 5). It is noteworthy that abundant taxa with porcelaneous and agglutinated tests, such as *Quinqueloculina* spp., *Spirosigmoilina* sp., *Borelis* sp. and *Textularia* spp., are observed in the calcareous mudstone of Sample QU-24, denoting a local lagoon environment (Murray, 1991).

4.3. Trace element and Nd isotope results

Results of trace element and Nd isotopic analyses of the silicate fraction of mudstones from the Isugod and Alfonso XIII Formations are listed in Tables S4. For elements that are common in felsic rocks, Rb and Y in the analyzed mudstones from the Isugod Formation show slightly higher concentrations than the Upper Continental Crust (UCC) (Rudnick & Gao, 2003), but Th, U, Nb, Zr and Hf show slightly lower concentrations than the UCC (Figure 6a). Abundances of the transitional elements, V, Sc, Co, Cr and Ni are slightly to significantly higher than the UCC. The trace element patterns of the analyzed mudstones from the Isugod Formation are generally consistent with the sandstones and mudstones from the Isugod Formation published by Cao et al. (2021), although the sandstones have lower concentrations of Rb, Th, U, Nb, Zr, Hf and Y (Figure 6a). The calcareous mudstones of the Alfonso XIII Formation share almost the same trace element pattern as the Isugod Formation samples except for significant higher abundances of U (Figure 6a). Chondrite-normalized distribution patterns of rare earth element (REE) concentrations in the Isugod and Alfonso XIII Formations (this study and Cao et al., 2021) are similar to those of the UCC with light REEs enrichment, heavy REEs depletion and a negative Eu anomaly (Figure 6b). However, it is also noteworthy that the Isugod and Alfonso XIII Formations show generally less relative enrichment in light REEs compared to the UCC (Figure 6b).

The $^{143}Nd/^{144}Nd$ ratios of the Isugod Formation mudstones are concentrated in the range from 0.512309 to 0.512338, corresponding to a ε_{Nd} range from -6.4 to -5.8 (Table S4). The $^{143}Nd/^{144}Nd$ ratios of the Alfonso XIII Formation mudstones are a bit lower than the Isugod Formation mudstones, varying from 0.512256 to 0.512316 and corresponding to a ε_{Nd} range from -7.4 to -6.3 (Table S4).

4.4. Heavy minerals and detrital zircon U-Pb geochronology

The percentages of non-opaque heavy minerals of four sandstone samples (QU-22a, QU-26a, QU-27a and QU-29a) from the Isugod Formation are listed in Table S5 and shown in Figure 7. The content of zircon varied from 4.4% to 54.9% of the total heavy mineral assemblage, and the content of tourmaline and rutile is in general lower than 0.6% and 5.4%, respectively (Figure 7). The relatively low ZTR index (zircon + tourmaline + rutile) in our samples is consistent with the data published by Suggate et al. (2014) and Cao et al. (2021), except for Sample PAL-55 (Suggate et al., 2014) that contains a high proportion of zircon (97.6%) (Figure 7). Nevertheless, the zircon-tourmaline-rutile assemblage indicates derivation from felsic rocks or recycling from older sedimentary units. The noteworthy content of Cr-spinel (19.9% and 85.4%) in Samples QU-22a and QU-26a and minor pyroxene (7.3%) in Sample QU-27a (Figure 7) indicate a basic-ultrabasic/ophiolitic provenance, in agreement with the dominance of the amphibole-Cr-spinel-pyroxene assemblage (74.0%–89.5%) in sample PAL-53, P024 and P025 (Cao et al., 2021; Suggate et al., 2014). Pyroxene grains from Sample QU-29a are highly weathered, probably due to the hot humid climate in this tropical region. This might explain why less durable minerals like pyroxene and olivine common in basic-ultrabasic rocks are rare or lacking in the samples with high content of Cr-spinel. There are abundant epidote (11.8%–47.8%) in samples QU-22a, QU-27a and QU-29a and minor garnet (8.5% and 8.7%) in samples QU-26a and QU-27a (Figure 7). Both garnet and epidote may be derived from a variety of source rocks, but most commonly are of metamorphic origin. Although kyanite indicative of high-grade metamorphic rocks was not observed in our samples, it was reported in Sample PAL-53 of Suggate et al. (2014).

The U-Pb ages of 371 new detrital zircon grains from samples QU-22a, QU-26a, QU-27a and QU-29a, in addition to 115 detrital zircon U-Pb ages of samples QU-26a and QU-27a published collectively by Yan et al. (2018) (Sample QU-26 in their Figure 6), are detailed in Table S6. Most zircon grains show oscillatory zoning (Figure S3) and Th/U ratios > 0.3 (Figure S4) which are typical of magmatic origin. Samples yielded a wide range of zircon U-Pb ages from 13 Ma to 3200 Ma. Zircons of Jurassic–Cretaceous age (66–200 Ma) make up 53%–68% of the total number of analyzed grains in these samples and generally fall into two age clusters of 80–150 Ma and 150–200 Ma (Figures 8a to 8d). Besides these two dominant Mesozoic clusters, there is also a significant age cluster of 200–300 Ma and two minor clusters of 600–1200 Ma and 1500–2300 Ma in Sample QU-22a (Figure 8a). There are also two minor age groups of 200–300 Ma and 1500–2300 Ma in Sample QU-26a (Figure 8b), three minor groups of 13–53 Ma, 200–300 Ma and 1500–2300 Ma in Sample QU-27a (Figure 8c), and several minor age clusters spanning 200–300 Ma, 300–500 Ma, 500–1000 Ma and 1500–2300 Ma in Sample QU-29a (Figure 8d). The minor but noteworthy Cenozoic group of zircons (13–53 Ma) presented in Sample QU-27a is also occasionally observed in other samples. Overall, it can be easily divided into two age clusters of 13–15 Ma and 30–53 Ma (Figure 8e).

5. Discussion

5.1. Biostratigraphic framework and subsidence history of the Isugod Basin

5.1.1. Biostratigraphic framework of the Isugod Basin

A robust depositional age model for the Isugod Basin is fundamental to constraining the timing and evolution of arc-continent collision between the Palawan microcontinental block and the Cagayan Ridge. Until now few biostratigraphic studies have been conducted on the Isugod Basin. Wolfart et al. (1986) tentatively estimated the Isugod Formation to be Middle Miocene in age without any microfossil age constraints. Aurelio & Peña (2010) mentioned the presence of Middle Miocene planktonic foraminifera in the Isugod Formation without providing any details. Aurelio et al. (2014) later regarded the Isugod Formation as the lateral equivalent of the Pagasa Formation offshore Palawan (Figure 9). The Pagasa Formation consists of Early–Middle Miocene silty to calcareous shales, claystones and calcareous sandstones (Hinz & Schlüter, 1985). The Pagasa Formation was offscraped in the front of the Palawan wedge during collision (Steuer et al., 2013) (Figure 1d). The top of the Pagasa Formation has been various estimated at 15.2 Ma (Steuer et al., 2013) and 12 Ma (Aurelio et al., 2014) without any definitive evidence. Ilao et al. (2018) looked at the well correlation data provided by Steuer et al. (2013), including two wells (Murex-1 and Paz-1) offshore southern Palawan and two wells (Busuanga-1 and Cadlao-1) offshore northwesternmost Palawan, and suggested that the top of the Pagasa Formation is diachronouns and appear to range between top of Zone N8 (~15.1 Ma) and top of Zone N14 (~10.5 Ma). We concur with Ilao et al. (2018) that the highly variability in age of the top of the Pagasa Formation may reflect biostratigraphy and formation identification issues. The top of the Pagasa Formation was not discussed in the text in Steuer et al. (2013) and what they provided in the correlation chart of selected well (their Figure 4) was a low resolution biostratigraphy with only the top of planktonic foraminiferal zones indicated. Moreover, the information of sampling history, such as whether the biostratigraphy data was collected directly from the Pagasa Formation or the sediments above, and from a sidewall core sample or a drill cutting sample were largely unknown. As marked in the well correlation chart of Steuer et al. (2013), there is an uncertainty in identifying the top of the Pagasa Formation in some wells, such as well Paz-1 offshore southernmost Palawan. In well Murex-1 offshore southern Palawan, there was a divergence on placing the top of the Pagasa Formation between Steuer et al. (2013) and Ilao et al. (2018). Diachronism of the top of the Pagasa Formation would be expected as the outward propagation of thrust front; however, this is difficult to evaluate because the sparsely distribution of the wells and in fact the Palawan wedge did not develop in the wells offshore northwesternmost Palawan. Luan & Lunt (2022) recently reviewed the unpublished report of the commercial wells offshore southwestern Palawan and provided detailed information of biostratigraphy and lithology of the wells. Based on this the top of the Pagasa Formation was placed near Zones NN5/NN6 boundary (13.5 Ma) in well Aboabo-1, and near Zones N11/N12 boundary (13.4 Ma) in wells Paragua-1 and Kamonga-1. Therefore, we consider that an age of ~13.4 Ma for the top of the Pagasa Formation would be more convincing.

Our biostratigraphic work, integrating planktonic foraminifera and calcareous nannofossils, dates the Isugod Formation to the Late Miocene (Zones N14–N16 or Zones NN7–NN9, 11.5–9.5 Ma). It is consistent with the youngest age population (13–15 Ma with peak age of 13.8 Ma) obtained from the detrital zircon which provides the maximum depositional age for the Isugod Formation (Figure 8e). The biostratigraphic result thus provides a solid age constraint for deposition of the Isugod Formation. Our work does not support a correlation between the Isugod and Pagasa Formations. Instead, the Isugod Formation is considered correlative to the lower part of the coarse-grained Matinloc

Formation (base at Zone N14, Williams et al., 1997) which uncomfortably overlies the fine-grained Pagasa Formation (Steuer et al., 2013) (Figures 1d and 9). The unconformity separating the Pagasa Formation from the Matinloc Formation was recognized on a regional scale, offshore the entire Palawan Islands. It is known as the Middle Miocene Unconformity or the Red Unconformity (Hinz & Schlüter, 1985) and has been tied to the collision of the Palawan microcontinental block with the Cagayan Ridge (Aurelio et al., 2014). On top the Palawan wedge, the Lower Matinloc Formation is represented by a fine sandy and clayish succession with a greatest thickness of ~200 m below the Tabon/Likas Limestone in the Upper Matinloc Formation (Steuer et al., 2013). It might be originated from the onshore area further toward the east (Steuer et al., 2013). In places, this succession has been subjected to syn-sedimentary folding and thrusting, and was recognized as a syn-thrust sequence (Aurelio et al., 2014; Ilao et al., 2018). The progradational units between the deformed wedge and the base of the Tabon Limestone observed between the nearshore edge and Island of Palawan from the seismic profile (Ilao et al., 2018) might be also ascribed to the Lower Matinloc Formation. The Lower Matinloc Formation seems not laterally continuous on top of the Palawan wedge and its distribution highly depends on the paleotopography of the uplifting wedge (Ilao et al., 2018; Luan and Lunt, 2022). It is absent in many places probably because it onlaps preexisting highs (Ilao et al., 2018). In this case, the Pagasa Formation of the deformed wedge might be capped by condensed sedimentation equivalent to the Lower Matinloc Formation or be directly capped by the Tabon Limestone, and then the base of the Tabon Limestone might be merged into the Red Unconformity. Age constraints of the Red Unconformity have largely depended on the top of the Pagasa Formation (e.g. Ilao et al., 2018; Luan & Lunt, 2022) probably because the base of the Matinloc Formation is more difficult to accurately date. Our biostratigraphy result of the Isugod Formation might help to constrain the unconformity to 13.4–11.5 Ma. Because the Matinloc Formation represents wedge-top deposits, we also interpret the Isugod Basin as a wedge-top basin overlying the Palawan wedge.

The depositional age of the Alfonso XIII Formation is disputed. Wolfart et al. (1986) assigned it to the Late Miocene (Figure 9) primarily based on larger benthic foraminifera and calcareous nannofossils, whereas Rehm (2003) proposed a late Early Miocene–Middle Miocene depositional age based on larger benthic foraminifera and planktonic foraminifera identified from thin section. However, precise taxonomic identification of foraminifera in thin section, whether larger or smaller ones, is always difficult. It is worth mentioning that Sr isotope dating of three unaltered oyster shells collected from different levels of the Alfonso XIII Formation by Rehm (2003) yielded younger ages of 9–6 Ma. However, this result was excluded by the author and attributed to contamination of minor terrigenous input. Our integrated microfossil analysis confirms the Late Miocene age of Wolfart et al. (1986) for the Alfonso XIII Formation and refines it to Zones N16–N17B (8.9–5.6 Ma). It also implies that the result from Sr isotope dating (9–6 Ma) of Rehm (2003) is reliable. Another piece of evidence is that if contamination of terrigenous input could alter $^{87}Sr/^{86}Sr$ ratio of the carbonate, it would lead to higher $^{87}Sr/^{86}Sr$ ratio and thus older ages considering that the contribution of material from the Palawan Ophiolite as we will discuss in Section 5.2. The Alfonso XIII Formation is almost coeval with the offshore Tabon/Likas Limestone in the upper Matinloc Formation (9.2–5.5 Ma) (Steuer et al., 2013) (Figures 1d and 9). The Tabon

Limestone is a continuous unit overlying the lower Matinloc Formation and the Palawan wedge in front of central and southern Palawan (Steuer et al., 2013). It was firstly considered as shallow marine carbonates (Steuer et al., 2013) but was later regarded as a condensed deep marine sedimentation (hemi-pelagic marl) in most of the offshore area which only approach a reefal facies nearshore Palawan (Luan and Lunt, 2022). Anyway, it represents a phase of starvation in terrigenous siliciclastics. The base of the Tabon Limestone was well dated around 9.2 Ma in three wells offshore central and southern Palawan, but was dated as young as ~7.8 Ma and ~6.8 Ma in other two wells (Steuer et al., 2013). The latter might be due to that the biostratigraphy data of these wells was obtained from drill cutting samples (Luan and Lunt, 2022) prone to be contaminated with fossils from shallower stratigraphic levels. The short age gap (~0.6 m.y.) between the Isugod and Alfonso XIII Formations (Figures 4 and 9) may represent either a hiatus/unconformity or merely represent the resolution of dating.

5.1.2. Subsidence of the Isugod Basin and gravitational collapse of the Palawan wedge

Evidence of sedimentology and benthic foraminifera indicates that the depositional paleobathymetry of the Isugod Formation increased upwards from <50 m in the basal limestone to a middle bathyal depth (600–1000 m) in the overlying turbidite sequences (Figure 5). The basal limestone located on the Eocene Central Palawan Ophiolite indicates that the forearc basement of the Cagayan Ridge had approached sea-level at that time owing to its obduction onto the distal margin of the buoyant Palawan microcontinental block. The turbidite sequences overlying the basal limestone of the Isugod Formation indicate a sudden increase in water depth, of more than ~500 m at ~11.5 Ma in the Isugod Basin, which led to drowning of the limestone platform followed by rapid siliciclastic sediment influx. The sudden increase in water-depth exceeded levels associated with global eustatic sea-level change (Miller et al., 2020) and therefore, we deduce that the sudden increase in water depth reflected rapid tectonic subsidence in response to arc-continent collision.

Although no normal faults bounding the Isugod Basin was directly observed in the field, a series of NE-SW striking seaward normal faults developed during two phases of gravitational collapse of the external part of the Palawan wedge and have been observed in offshore seismic profiles to the northwest of the Isugod Basin (Ilao et al., 2018). The early normal faults, sealed by the Matinloc Formation, only affected the wedge and have been interpreted as gravity-driven structures responding to collisional thickening-related uplift. In contrast, the later normal faults offset not only the top of the wedge but also the overlying Matinloc Formation (including the Tabon/Likas Limestone) and have been assumed to result from post-collisional gravitational collapse when the effects of compressional deformation on the wedge had largely ended (Ilao et al., 2018). The subsidence of the Isugod Basin might be associated with the early normal faulting and gravitational collapse the Palawan wedge during the collision stage. This would not be surprising because gravitational collapse of an accretionary/orogenic wedge often occurs during the subduction-collision process (e.g. Platt, 1986), even though post-collisional gravitational collapse is a more common feature in collisional orogenic belts (e.g. Dewey, 1988; Platt & Vissers, 1989).

Some evolutionary models of accretionary wedges predicted that large-scale tectonic underplating beneath the wedge may uplift the underplated and overlying rocks, oversteepen the wedge taper and eventually result in gravitational collapse and extensional tectonics above the affected region (e.g. Platt, 1986; Underwood & Moore, 1995). This mechanism for gravitational collapse has been well documented in the Makaran accretionary wedge (Ruh, 2017; 2020) and the Hikurangi-Kermadec forearc (New Zealand) (Sutherland et al., 2009). This tectonic process might also occur during the arc-continent collision, when the passive continental margin was underthrust and could be in part underplated beneath the orogenic wedge. This would act a major agent for crustal thickening and orogenic growth (e.g. Simoes et al., 2007; Harris, 2011). The syn-orogenic basins developing on the Timor wedge, where the Australian continental margin underthrust beneath the Banda forearc, have been interpreted to result from local gravitational collapse of the wedge triggered by subsurface underplating and duplexing in response to the arc-continent collision (Tate et al., 2014). The Miocene Cilento wedge-top basin in the southern Apennines, where the Calabrian arc has collided with the Apulian/Adria continental margin, was interpreted as the result of syn-orogenic extension linked to gravitational instability of a vertically growing orogen (Corrado et al., 2019). Analogously, the Isugod Basin might also be formed by local extensional gravitational collapse of the wedge, after underthrusting of the continental margin beneath the Central Palawan Ophiolite (Figure 1d). Extension would have been triggered by regional uplift of the forearc (i.e. the hinterland of the orogenic wedge and the forearc ophiolite) due to large-scale underplating of continental margin rocks. The pebbly mudstone mass wasting deposits in the lower part of the Isugod Basin might represent a response to the gravitational collapse, probably transported by debris flow across a steep and unstable slope (fault scarp), from the uplifted wedge to the subsiding deep-water basin. Small bodies of the Panas-Pandian Formation and the Ransang Limestone were mapped by Wolfart et al. (1986) and Aurelio et al. (2014) in the Isugod Basin, although they were not observed during our field investigation. We suspect that they might represent large exotic blocks slumped from the uplifted wedge. The underplated continental margin sedimentary rocks might be represented by the Barton Group, with moderately high pressure-low temperature metamorphism (Suzuki et al., 2000). It was buried within the core of the wedge but has been widely exhumed in northern Palawan (Keenan, 2016). The overall structure of the Barton Group exhibits a slightly overturned, north-northwest verging anticline, and the Caramay Schist (the unit underwent highest grade metamorphism in the Barton Group) crops out in the core of the anticline (Mitchell et al., 1986; Keenan, 2016; Padrones et al., 2017). We inferred that this structure might result from underplating in the form of tectonic antiformal stacking of coherent thrust sheets. The transition from deep-water turbidites of the Isugod Formation to the overlying shallow-water Alfonso XIII Formation at 9.5–8.9 Ma can be interpreted as a response to continued tectonic uplift during arc-continent collision.

The presence of overpressured fluid-rich mudstones in the orogenic wedge was also proposed as a mechanism for the gravitational instability and collapse of the wedge and opening of syn-orogenic basins (Harris et al., 1998; Harris, 2011; Morley et al., 2023; Morley, 2024). For instance, the gravitational collapse of the Timor wedge can also be driven by lowering of the coefficient friction of the décollement at the base of the wedge as the décollement propagates into mud-rich units (overpressured mudstone) of the underthrust Australian continental margin (Harris et al., 1998; Harris, 2011), in addition to tectonic underplating. It is also noted that the shale-dominated Pagasa Formation in the external part of the Palawan wedge was inferred to have been highly overpressured in order to readily deform (Morley et al., 2023). We speculate that the overpressured mudstone of the Pagasa

Formation, probably occurring near the base of the Pagasa Formation/top of the Nido Limestone, might weaken the décollement and contribute to gravitational collapse of the external part of the wedge as observed from the seismic profile offshore central Palawan (Ilao et al., 2018). The presence of this overpressured mudstone may also explain the step up of the basal décollement from deeper levels below the Eocene Pulute Formation into the base of the Pagasa Formation/top of the Nido Limestone when the Pagasa Formation in the foreland was caught up in thrust belt deformation. The most prominent example of an upward propagation of a décollement from deeper level into the base of the foreland characterized by overpressured fine-grained deposits can be found in the frontal Himalaya (Chapman and Decelles, 2015). However, we doubt that weakening of the décollement by the overpressured mudstone would lead to the subsidence of the Isugod Basin as it is located directly on the Panas-Pandian/Pulute Formation and the Central Palawan Ophiolite (Figure 1d) based on the field observation. The Pagasa Formation, which was frontally accreted into the external part of the Palawan wedge, could not have been underthrust deep under the hinterland of the wedge where the Isugod Basin is located (Figure 1d). Morley et al. (2023) have traced the continuity of the external part of the Palawan wedge to the area offshore North Sabah, Borneo. The North Sabah wedge was characterized by the development of a serious of mini-basins with sediment thickness of 3–4 km (Morley et al., 2023). These mini-basins were proposed to be subsided by a combination of downbuilding and normal faulting driven by rapid sediment loading on the unstable, overpressured mudstone (equivalent of the Pagasa Formation) within the wedge (Morley et al., 2023; Morley, 2024). We argue against that the subsidence of the Isugod Basin was induced by the sediment loading on the wedge because there would be no overpressured mudstone (the Pagasa Formation) under the basin. In addition, sediment supply to the Isugod Basin (estimated thickness of ~ 800 m) was much less than that to the mini-basins offshore Sabah, due to the much smaller landmass in Palawan than Borneo. Finally, it is possible that subsidence driven by sediment loading might occur gradually, unlike the rapid subsidence from shallow marine condition (<50 m) to middle bathyal setting (600–1000 m) in the Isugod Basin. Above all, we do not rule out that overpressured mudstone of the Pagasa Formation also played an important role in gravitational collapse of the external part of the Palawan wedge. However, regarding the development of the Isugod Basin, we prefer that tectonic underplating beneath the orogenic wedge is a more plausible mechanism. It not only led to the subsidence of the basin to create accommodation space, but also uplifted and exposed the orogenic wedge subaerially to supply sediments (see Section 5.2). Coincidently, Morley et al. (2023) also proposed that early stages of the development of the mini-basin offshore Sabah (13–10.5 Ma) were probably related to underthrusting of the Dangerous Grounds crust below the North Sabah and Crocker wedges. We suggest that this might also involve a process of tectonic underplating.

We also note that during the early or immature stages of collision, the slab pull force of the subducting oceanic lithosphere might yield a trenchward retreat (i.e. the subduction rate exceeds the overall plate convergence) and cause regional extension within the upper plate and at the leading edge. Such rollback is well documented in the Mediterranean region (e.g. Royden et al., 1993) and the Banda arc-continent collision zone (Harris, 2003; 2006). However, the subsidence of the Isugod Basin may not be the product of large-scale regional extension, in view of the evidence for forearc uplift and the large terrigenous clastic supply into the basin (see Section 5.2).

5.2. Double provenance supply into the Isugod Basin

Once the Palawan wedge had been uplifted and exposed subaerially, one would expect that the deformed continental margin sedimentary rocks of the Palawan wedge and the emplaced Eocene Central Palawan Ophiolite would become the main sediment source to the Isugod wedge-top basin. Enrichment of Rb seen in the Isugod and Alfonso XIII Formations and their overall REE patterns are similar to those of the Palawan continental margin sequences, including the Middle Eocene–lowermost Oligocene Panas-Pandian Formation and the Upper Cretaceous Barton Group (Cao et al., 2021; Chen et al., 2021) (Figure 6), and suggest sediment supply by erosion from felsic rocks. These continental margin sequences were thought to be derived from the Cathaysia Block (SE South China) where Jurassic-Cretaceous granites are widespread (e.g. Chen et al., 2021; Shao et al., 2017). Because the Palawan microcontinental block drifted away from South China shortly after continental breakup at 33–32 Ma (Chen et al., 2021; Li et al., 2014), the eroded felsic material in the Isugod and Alfonso XIII Formations must be recycled from the Palawan continental margin sequences. Granites of diverse age outcrop in northern Palawan (e.g. Padrones et al., 2017) (Figure 1b) and are not expected to be the major felsic source for the Isugod and Alfonso XIII Formations owing to their limited outcrop area.

Enrichment of transitional elements in the Isugod and Alfonso XIII Formations is in contrast to rocks from the Palawan continental margin sequences, which have a lower abundance of transitional elements than the UCC (Figure 6a). They also show less enrichment in light REEs than the UCC and Palawan continental margin sequences (Figure 6b). These differences indicate additional input of basic-ultrabasic material in the Isugod and Alfonso XIII Formations, as implied from a Co/Th-La/Sc plot (Figure 10a), in which both formations reflect a mixture eroded from the Palawan continental margin sequences (Cao et al., 2021; Chen et al., 2021) and the Palawan Ophiolite (Gibaga et al., 2020; Keenan et al., 2016). In the La-Th-Sc and Th-Sc-Zr/10 ternary diagrams (Figures 10b and 10c), the Isugod and Alfonso XIII Formations plot between the continental and oceanic island arc settings, which also requires a contribution from the Palawan Ophiolite which represents an oceanic island forearc. However, it is not possible to ascertain whether the basic-ultrabasic fraction was derived from the Central or Southern Palawan ophiolites, because they are cluster together in Figures 10a–10c.

Until now, only limit Nd isotope data have been reported from the Palawan Ophiolite, including a basalt (ε_{Nd} =9.4) and a boninite (ε_{Nd} =5.4) from the Central and Southern Palawan Ophiolites, respectively (Gibaga et al., 2020). As for the continental margin sequences, Nd isotope data have only been reported from the Panas-Pandian Formation (Chen et al., 2021). Based on the data available, the ε_{Nd} values of the Isugod and Alfonso XIII Formations (-7.4 to -5.8) are much closer to those of the Panas-Pandian Formation (-9.3 to -8.3) than the Palawan Ophiolite (Figure 10d). However, this does not mean dominant erosion from the Palawan wedge, because the Panas-Pandian Formation has much higher Nd concentrations than the rocks of the Palawan Ophiolite (generally <10 ppm) (Chen et al., 2021; Gibaga et al., 2020; Keenan et al., 2016). We perform simple two-component mixing models based on Nd isotope ratios, involving the Palawan Ophiolite and the Panas-Pandian Formation. It can be seen that regardless of whether the Central or Southern Palawan Ophiolite are treated as the end-member, the proportion of sediment flux from the ophiolite would reach 40%–70% in the silicate fraction of the Isugod and Alfonso XIII Formations (Figure 10d).

Three types of heavy mineral assemblages was observed in Isugod Formation sandstones (this study and Cao et al., 2021; Suggate et al., 2014) (Figure 7). The presence of Cr-spinel, amphibole and pyroxene grains is consistent with a Palawan Ophiolite origin. The medium- to high-grade metamorphic minerals including epidote, garnet and kyanite could only be derived from the metamorphic sole of the Central Palawan Ophiolite (Keenan et al., 2016), documenting the existence of material eroded from the Central Palawan Ophiolite in the Isugod Formation. Garnet and kyanite are also common in high-pressure metasedimentary rocks in the late stages of metamorphism within a subduction zone owing to the subduction of oceanic crust materials and passive continental margins (e.g. Smye et al., 2010). However, no such units associated with an oceanic accretionary wedge have been found in Palawan. The Barton Group which may have originated from underplating of continental margin rocks beneath the orogenic wedge, only experienced very low to low grade metamorphism (Suzuki et al. 2000). Notable, even the Caramay Schist, which experienced the highest grade metamorphism in the Barton Group, is only composed of phyllite to low grade schist (Suzuki et al. 2000). Therefore, the Barton Group could not supply the medium- to high-grade metamorphic minerals for the Isugod Formation. The zircon-tourmaline-rutile assemblage, indicative of felsic source rocks, might be recycled from the Panas-Pandian Formation or the Barton Group because of the very high ZTR index of these units (Cao et al., 2021; Chen et al., 2021; Shao et al., 2017; Suggate et al., 2014) (Figure 7).

To better constrain the source area of the detrital zircons in the Isugod Formation, the traditional visual comparison of age spectra was further added by using nonmetric multidimensional scaling (MDS) (Vermeesch, 2013) in Figure 8. The MDS maps group samples with similar age spectra and pull apart samples with different spectra (Vermeesch, 2013). Previous U-Pb dating of detrital zircons from the Isugod Formation sandstones, including samples PAL-55, P024 and P025 (Cao et al., 2021; Suggate et al., 2014) (Figure 8f) collected near Site QU-26 show a unimodal age distribution resembling the Barton Group (Shao et al., 2017; Suggate et al., 2014; Walia et al., 2012) (Figures 8h, 8i and 8j). The proportion of Jurassic–Cretaceous zircons is as high as ~77%. Based on these results the detrital zircons in the Isugod Formation are interpreted to be recycled from the Barton Group (Cao et al., 2021; Suggate et al., 2014). However, our samples (QU-22a, QU-26a, QU-27a and QU-29a) collected from across a wider area generally contains a lower percentage of Jurassic–Cretaceous zircons (~60%) and higher percentages of zircons older than 200 Ma (~35%) (Figures 8a to 8e). They have a closer affinity to the Panas-Pandian Formation, which contains a lower proportion of Jurassic–Cretaceous zircons (55%) (Chen et al., 2021; Shao et al., 2017; Yan et al., 2018) (Figures 8g and 8i). This is especially true when the two young age groups (13–15 Ma and 30–52.5 Ma) in the Isugod Formation are excluded (Figure 8j). Therefore, we argue that the detrital zircons in the Isugod Formation were more likely recycled from the Panas-Pandian Formation than from the Barton Group. Although the Isugod Formation generally exhibits a lower proportion of Mesoproterozoic–Paleozoic (300–1500 Ma) detrital zircons (11%) (Figure 8e) than the Panas-Pandian Formation (27%) (Figure

8g), this may be partly result from sampling bias because the proportion of Mesoproterozoic–Paleozoic zircons can also reach up to 26% in Sample QU-29 from the Isugod Formation (Figure 8d). To minimize sampling bias, analyses of more Isugod Formation samples collected from across a much wider area is necessary in the future work.

Suggate et al. (2014) also found a small number of zircons dated to 36–49 Ma in the Isugod Formation and proposed the Middle Eocene Central Palawan granite (42±0.5 Ma) intruding the Barton Group as their likely source. However, we propose that the 31–52.5 Ma zircons (Figure 8e) were derived from the Central Palawan Ophiolite which is known to contain zircons dating to ~34.1 Ma and ~40.5 Ma (Dycoco et al., 2021; Keenan et al., 2016) given its proximity to the Isugod Basin. There are additional two lines of evidence that support this interpretation. Firstly, the 31–52.5 Ma zircons have U contents (average of 235 ppm, n=14) (Table S6) similar to those reported from the Central Palawan Ophiolite (average of 222 ppm) (Dycoco et al., 2021; Keenan et al., 2016), but much lower than those reported from the Central Palawan granite (average of 646 ppm) (Suggate et al., 2014). Secondly, these zircons show no or only weakly, broadly zoning under cathodoluminescence (Figure A3), which is more typical in igneous zircon from mantle-derived rocks (Rubatto & Gebauer, 2000). As for the 13–15 Ma zircons first reported here, these grains might be associated with the volcaniclastic sediments of Zone NN5 (13.5–14.9 Ma) generated by Cagayan Ridge volcanism and drilled at ODP Site 771, SE Sulu Sea (Rangin & Silver, 1991). Potentially, such volcaniclastic sediments might be also deposited on the forearc ophiolite basement (being part of the NW Sulu Sea) and then recycled to the Isugod Basin when the ophiolite basement was finally exposed subaerially owing to obduction.

As the Panas-Pandian Formation represents the sedimentary cover of the Palawan wedge, in contrast to the Barton Group which was buried at depth in the wedge, it must have been the first to be uplifted and exposed subaerially (probably in northern Palawan) during the arc-continent collision. The simultaneous presence of materials eroded from both the Panas-Pandian Formation and the Central Palawan Ophiolite into the Isugod Basin implies uplift and emergence of the Palawan wedge and forearc ophiolite (Figure 13d). This occurred because of the obduction of the Central Palawan Ophiolite over the Palawan wedge. Such a scenario is consistent with our preferred model of subsidence of the Isugod Basin due to local extensional collapse in response to forearc uplift. Although sediment recycling could have taken place when the wedge was still submarine, subaerial exposure is inferred from the subrounded to rounded character of the pebbles and the presence of coal lenses and amber (Aurelio & Peña, 2010) reported in the pebbly mudstones. It is also implied by the widespread appearance of migrating submarine canyons above the Red Unconformity offshore Palawan separating the Pagasa Formation from the Matinloc Formation (Franke et al., 2011; Tong et al., 2019). Thus, our observation from the Isugod Basin confirms that the unconformity was produced by the arc-continent collision (Aurelio et al., 2014) although little has been known about the lithology and provenance of the offshore strata below and above the unconformity.

The supply of syn-collisional sediments from two sources in Palawan differs from the syn-collisional sediment in Taiwan that almost entirely eroded from the orogenic wedge with little contribution from the colliding Luzon arc-forearc basement (e.g. Chen et al., 2017; Clift et al., 2003). This difference might reflect from that the Luzon arc-forearc was not obducted over but instead bulldozed into the South China margin strata, with much of the shortening occurring by inversion of the continental margin (Ryan & Dewey, 2019). In contrast, the forearc of the Cagayan Ridge was obducted over the Palawan continental margin. This is more similar to New Guinea and Timor where the obducted arc-forearc made an important contribution to the syn-collisional sediments (Abbott et al., 1994; Duffy et al., 2017).

5.3. Implication for the evolution of arc-continent collision in Palawan

5.3.1 Timing of onset of arc-continent collision in Palawan

Our provenance results indicate that since ~11.5 Ma there was concurrent derivation of eroded materials into the Isugod Basin from the Panas-Pandian Formation with a continental affinity and the Central Palawan Ophiolite representing the obducted forearc basement from the upper plate. This indicates impingement between the Palawan microcontinental block and the Cagayan Ridge. A mixture of both components derived from the Buruanga Peninsula being part of the Palawan microcontinental block and from the volcanic rocks of the Antique Range which represent the onshore extension of the Cagayan Ridge (Bellon & Rangin, 1991) is also reflected in the clastic rocks of the Frangante Formation in northwestern Panay (Gabo et al., 2009). Therefore, the mixture of both continent-derived and arc-derived components in the Frangante Formation also indicates the juxtaposition of the Palawan microcontinental block and Cagayan Ridge. The Frangante Formation was assigned a Middle Miocene depositional age based on larger foraminifera in the limestone patches intercalated with pyroclastic and lava flow deposits overlain by clastic rocks (Aurelio & Peña, 2010). However, zircons separated from a tuffaceous sandstone gave a youngest age of 11±1 Ma (Walia et al.,

2013) that represent the maximum depositional age of the clastic rocks of the Frangante Formation. This means it was almost coeval with the deposition of the Isugod Formation. This scenario hints at a contemporaneous arrival of syn-collisional sediments in central-southern Palawan and northwestern Panay in the Late Miocene and probably a simultaneous arc-continent collision along the collision boundary. The oldest syn-collisional sediments in the Isugod Basin (~11.5 Ma) provide a youngest limit for the onset of arc-continent collision, requiring collision before ~11.5 Ma.

Although Rangin & Silver (1991) proposed a Middle Miocene age (~16 Ma) for cessation of arc volcanism based on the top of pyroclastic rocks at ODP Site 768 in the SE Sulu Sea (Figure 1a), this is not a good indicator of collision initiation. Evidence of younger arc volcanism can be observed from the southeastern flank (ODP Site 771, 13.5–14.9 Ma, Rangin & Silver, 1991) and the crest (10.7±1.5 Ma, Kudrass et al., 1990) of the Cagayan Ridge. Moreover, arc volcanism might continue several million years after collision initiation, as observed in Banda arc north of Timor (Harris, 2011), making it unreliable for constraining the timing of collision initiation.

Based on the top of the Nido Limestone (carbonate platform) underthrust beneath the external part of the Palawan wedge, Steuer et al. (2013) suggest that the onset of thrusting of the Palawan wedge did not start before ~18 Ma. We doubt that onset of thrusting of the Palawan wedge, even its external part, could be exactly dated by the top of the Nido Limestone. The top of the Nido Limestone acts as a décollement beneath the external part of the wedge, might only implies that imbricate thrusting (frontal accretion) above the décollement should be sometime rather than immediately after the end of deposition of the

Nido Limestone. In addition, it would be expected that the onset of the thrusting in the internal part (hinterland) of orogenic wedge, which marks the initiation of collision might be older than that in the external part of the orogenic wedge, owing to the propagation of the thrust front toward the foreland. Evidence from the onshore equivalents of the Nido Limestone incorporated into the internal part of the orogenic wedge show that the thrusting was not much older than ~18 Ma (Wolfart et al., 1986; Rehm, 2002). The St. Paul Limestone just north of the Ulugan Bay Fault (Figure 1b) contains larger foraminifera of *Lepidosemicyclina thecideaeformis Rutten* (Wolfart et al., 1986) indicative of Burdigalian age (Early Miocene) (BouDagher-Fadel, 2018), suggesting that at least the youngest part of the limestone should extend to 20–16 Ma. The small body of the Ransang Limestone enclosed in the Isugod Basin (i.e. Taglupa profile of Rehm, 2002) (Figure 1c) contains *Miogysinoides* and *Flosculinella bontangensis* (Rutten), suggesting an age of Letter Stages Lower Tf1 (planktonic foraminiferal zone N7, 17.5–16.4 Ma). If taking this limestone body into consideration, the thrusting in the hinterland of the Palawan wedge should not commence before ~17.5 Ma. Given the difficulty and complexity of directly dating the thrusting in the Palawan wedge, we prefer to constrain the timing of the onset of the arc-continent collision from a perspective of foreland evolution. The transition from the shallow marine Nido carbonate platform to the basinal Pagasa Formation clastics was often interpreted as the result of foreland flexural subsidence driven by the thrust-sheet loading in the orogenic wedge (e.g. Steuer et al., 2014; Ilao et al., 2018). Therefore, the regional drowning of the Nido carbonate platform at ~18 Ma might record the onset of arc-continent collision between the Palawan microcontinental block and the Cagayan Ridge. This timing (~18 Ma) do not largely conflict with the oldest possible age of the youngest Nido Limestone (17.5 Ma) incorporated into the hinterland of the wedge.

Until now few studies have been focused on the lithology and provenance of the Early–Middle Miocene Pagasa Formation accumulated in response to the foreland flexural subsidence when arc-continent collision in Palawan initiated (as we have discussed above). In light of Aurelio et al. (2014) and Steuer et al. (2014), the shale-dominated Pagasa Formation was mainly derived from northern Borneo, where a large landmass had been exposed, rather than an orogenic wedge in Palawan. It is noteworthy that frequent reworked Eocene microfossils has been reported from the Early–Middle Miocene Pagasa Formation (Ilao et al., 2018; Luan and Lunt, 2022). They were supposed to be originated from the Eocene–Lower Oligocene Panas-Pandian/Pulute Formation of the Palawan wedge, because reworked Eocene microfossils are absent from the coeval shale units (Setap and Stage III Shales) proximal to northern Borneo (Lunt et al., 2022). However, rare microfossils could be extracted from the Panas-Pandian Formation exposed onland central and southern Palawan due to severe tropical weathering (Wolfart et al., 1986; Chen et al., 2021). For the same reason, Eocene reworked microfossils are seldom observed from the Isugod Basin sediments recycled from the Panas-Pandian Formation. We deduced that the reworked Eocene microfossils might be introduced into the Pagasa Formation through submarine erosion from a growing wedge (probably submerged) to avoid the intense tropical weathering. In this sense, the earliest syn-orogenic sediments should be represented by the Early–Middle Miocene Pagasa Formation instead of the Late Miocene Isugod Formation.

An Early Miocene age (~20 Ma) for collision onset in Palawan was proposed by Hall

(2013) based on the sedimentary record from the Tajau Sandstone Member (lower member of the Kudat Formation) of northernmost Sabah. The Early Miocene age for the Tajau Sandstone Member was assigned based on biostratigraphic study of Clement & Keij (1958). These rocks contain kyanite and garnet grains that were thought to solely come from the high-grade metamorphic sole of the Central Palawan Ophiolite (Hall, 2013; van Hattum et al., 2013; Suggate and Hall, 2014). In addition, the sparse paleocurrent data from the Tajau Sandstone Member indicated that the source area may have been in the north, perhaps from Palawan or from the currently submerged area between Palawan and northern Sabah (Tongkul, 1994; van Hattum, 2005). Accordingly, Hall (2013) dated the beginning of collision in Palawan as Early Miocene (~20 Ma) and suggested a short-lived orogenic belt, much wider than Palawan today, that later (after ~16 Ma) collapsed by subduction rollback of the Celebes Sea.

However, several lines of evidence argue against the sediment supply from an orogenic belt in Palawan to the Tajau Sandstone Member in Sabah in the Early Miocene (~20 Ma). First of all, the depositional age of the Tajau Sandstone Member remained controversial. Lunt & Madon (2017) re-evaluated the larger benthic foraminifera reported by Clement & Keij (1958) and found that thirty of the samples are Late Oligocene in age with only five samples dating to the Early Miocene. Rahim et al. (2017) conducted a new biostratigraphic study on the Tajau Sandstone Member and discovered Early–Middle Eocene calcareous nannofossils, planktonic foraminifera and larger foraminifera from several outcrops, suggesting that these outcrops are of Early–Middle Eocene age. If we interpret these Early–Middle Eocene outcrops as exotic blocks originating from older sedimentary rocks, then the Tajau Sandstone Member should be dated as Late Oligocene–Early Miocene rather than Early Miocene.

However, an orogenic belt in Palawan since the Late Oligocene largely diverges from the onset of collision at ~18 M and the subsequent emergence of the Palawan wedge and the obducted ophiolite at ~11.5 Ma based on our geologic observation. Furthermore, timing of the obduction of the Central Palawan Ophiolite onto the Palawan continental margin could be constrained between 20–16 Ma and ~11.5 Ma by the underlying St. Paul Limestone (top at 20–16 Ma) (Wolfart et al., 1986) and the overlying Isugod Formation (base at ~11.5 Ma), and could not be as early as Late Oligocene.

It is noted that obduction of the forearc ophiolite can also occur when a classic accretionary wedge grows beneath the ophiolite during oceanic subduction (Wakabayashi and Dilek, 2003). However, it seems unlikely that an accretionary prism would develop during the intra-oceanic subduction stage in Palawan, which requires the thickness of sediments accumulated in the trench exceeding ~1 km (Clift and Vannucchi, 2004). Furthermore, no classic accretionary wedge has been identified within the Palawan wedge. Therefore, we do not expect the obduction of the Central Palawan Ophiolite onto an accretionary wedge during this stage, nor would there be an emergent accretionary wedge in Palawan to supply sediments to the Tajau Sandstone Member in the Late Oligocene. In contrast, a large accretionary wedge primarily composed of the Late Eocene–Oligocene Crocker Formation (i.e. the Crocker accretionary wedge) was well developed around northern Borneo, owing to sufficient sediment supply from the upper plate (van Hattum et al., 2013). Ophiolites are widespread in Sabah, and a recent study suggested that most of the ophiolites are of Triassic to Cretaceous age (185–85 Ma) and were generated in a forearc setting related to the Mesozoic Paleo-Pacific subduction (Wang et al., 2023). However, there are also ophiolite of

Eocene age (47–42.5 Ma) that might be correlated to the Central Palawan Ophiolite (Chien et al., 2019) and ophiolite of Late Miocene age (10.5–9.2 Ma) that might be related to the opening of the SE Sulu Sea (Tsikouras et al., 2021). In general, the Sabah ophiolites were directly obducted onto the Crocker accretionary wedge but not the deformed continental margin of the Dangerous Grounds. Therefore, we expected that the obduction of the Sabah ophiolites onto the Crocker accretionary wedge might have occurred during the subduction of the Proto-SCS. Although outcrops of metamorphic sole of the Sabah ophiolites has not been directly observed, blocks of garnet-pyroxenite and garnet-kyanite amphibolite have also been reported in Miocene conglomerates from eastern Sabah (Omang and Barber, 1996; Parkinson et al., 1998). These blocks were considered to be derived from the metamorphic sole of the Sabah ophiolites (Omang and Barber, 1996). Consequently, it is plausible that kyanites and garnets in the Tajau Sandstone Member also originated from such a metamorphic sole of the Sabah ophiolites.

Considering the southward paleocurrents in the Tajau Sandstone Member, we suggest that the currently submerged area between Palawan and northern Sabah (but still with some islets dominated by the Sabah ophiolites), as alternatively proposed by van Hattum (2005), might be a more probable provenance for the Tajau Sandstone Member. There was likely an emergent Crocker accretionary wedge obducted by the Sabah ophiolites during the Late Oligocene in this area. This very nearby source could also explain the presence of the olivine, one of the least stable heavy minerals, in the Tajau Sandstone Member (van Hattum et al., 2005). Olivine is even not found in the Late Miocene Isugod Basin (Figure 7) though it is proximal to the Central Palawan Ophiolite. It is puzzling that the Tajau Sandstone Member contain an obviously higher proportion of Jurassic zircons (~26% of the total) than the Late Eocene–Oligocene Crocker Formation (~10% of the total) (van Hattum et al., 2013; Suggate and Hall, 2014). The Jurassic zircons in the Tajau Sandstone Member are unabraded, and they were interpreted as the first-cycle zircons from Jurassic granites on the Palawan microcontinental block (van Hattum et al., 2013; Suggate and Hall, 2014). However, no Jurassic granites has been found in Palawan. Recently, Jurassic tonalities associated with the Sabah ophiolites has been reported from the Segama Valley region, eastern Sabah (Burton-Johnson et al., 2020). Potentially, similar units in Sabah might provide the unabraded Jurassic zircons for the Tajau Sandstone Member.

The collision in Palawan initiated at ~18 Ma (Figure 11 c) and postdated the collision in Sabah (northern Borneo) that may have begun as early as ~23 Ma (Figure 11b) (Hall, 2013; van Hattum et al., 2013; Lunt, 2022). This configuration implies that the collision propagated eastward along the southern SCS margin (Figure 1a and 11), possibly reflecting the irregular shape of the blocks rifted away from the South China margin, with a narrower Proto-SCS in the west compared to the east (Figure 11a). The collision occurred in Boneo and Palawan might finally lead to the cessation of the seafloor spreading of the SCS at 16–15 Ma (Morley, 2016; Savva et al., 2014; Taylor and Hayes, 1983) (Figure 11d).

5.3.2. A significant uplift pulse in the late stage of arc-continent collision

The Red Unconformity/Middle Miocene Unconformity, which separates the Matinloc Formation from the Pagasa Formation (as the external part of the Palawan wedge) offshore Palawan (13.4–11.5 Ma) (Figures 1d and 9), was traditionally viewed as a major collision event in response to the arc-continent collision between the Palawan microcontinental block and the Cagayan Ridge (Aurelio et al., 2013, 2014; Sales et al., 1997; Williams et al., 1997). However, Luan and Lunt (2022) proposed that the Red Unconformity resulted from the end of thrusting of the Palawan wedge, leading to an abrupt pause in uplift of the wedge. This interpretation is primarily supported by the highly condensed sedimentation (Matinloc Formation) overlying the shale-dominated Pagasa Formation with stratigraphic reworking of microfossils, suggesting a sudden decrease in sedimentation rate across the unconformity (Luan and Lunt, 2022). As previously mentioned, the reworked Eocene microfossils in the Pagasa Formation might indicate erosion from the submerged Palawan wedge, but this does not necessitate a rapid sedimentation rate for the shale-dominated Pagasa Formation. Moreover, a big issue with the interpretation of Luan and Lunt (2022) is their neglect of the presence of the coarse-grained Lower Matinloc Formation and their treatment of all the Matinloc Formation as condensed sedimentation similar to the Tabon Limestone (Upper Matinloc Formation). This oversight may be attributed to the fact that the studied wells, such as well Aboabo A-1x and Baragatan-1A (Ilao et al., 2018; Luan and Lunt, 2018), tend to be located on the relative topographic highs on the Palawan wedge. Given the presence of the Lower Matinloc Formation, we argue against Luan and Lunt (2022) that the Red Unconformity and the base of the Tabon Limestone (Lower/Upper Matinloc Formation Unconformity) should be combined as a single unconformity. The Lower Matinloc Formation is characterized by a fine sandy and clayish succession with a maximum thickness of ~200 m on the external part of the wedge (Steuer et al., 2014) and may encompass the syn-thrust sequences and progradational units reported by Ilao et al. (2018). In the Isugod wedge-top basin, the Lower Matinloc Formation (Isugod Formation) is primarily composed of pebbly mudstone and sandstone-mudstone interbeds with an estimated thickness of ~800 m. This sediment distribution pattern suggests that the siliciclastic influx from the hinterland of the Palawan wedge (which includes its sedimentary cover and the obducted ophiolite in northern Palawan) was primarily accumulated on the subsided wedge-top basin and also progradated into the topographic low on the external part of the wedge. This scenario is consistent with a significant uplift pulse in the hinterland of the Palawan wedge, as proposed by Ilao et al. (2018) for the origin of the gravity-driven structures offshore central-southern Palawan. This is further evidenced by the Matinloc Formation offshore northwestern Palawan which primarily consist of a polymictic conglomerate with an interval of sandstone at the base (Sales et al., 1997; Williams et al., 1997). Consequently, we infer that the Red Unconformity marks the onset of the uplift pulse of the Palawan wedge. This process not only led to the gravitational collapse of the Palawan wedge and subsidence of the Isugod Basin, but also contributed to the subaerial exposure of the Palawan wedge and obducted forearc ophiolite. This, in turn supplied siliciclastic sediments for the Isugod Basin (Isugod Formation) and other topographic lows on the Palawan wedge (Lower Matinloc Formation).

As the continental margin is underthrust beneath the orogenic wedge, uplift driven by tectonic underplating at depth through duplexing and antiformal stacking of the continental crust and sedimentary cover, and facilitated by surface erosion, may lead to exhumation of deep rocks (Malavieille et al., 2021). The Middle-Late Miocene age (13.4–11.5 Ma) proposed here for the onset of the significant uplift pulse in the late stage of arc-continent collision is supported by the exhumation event of metamorphic and intrusive rocks (~11 Ma) in northern Palawan. A whole rock K/Ar age of 10.5±0.6 Ma associated with uplift cooling was reported from biotite schist of the Barton Group (Mitchell et al., 1986). Zircon and apatite U-Th/He ages from the Middle Miocene Kapoas Granite north of the Barton Group show rapid cooling had commenced at ~11 Ma and continued at an average rate of ~70–75℃ until ~8.5±0.4 Ma (Foster et al., 2015). Exhumation events at ~12–11 Ma are also reported from the eastern edge of the Palawan microcontinental block (Dimalanta et al., 2009; Walia et al., 2013). Zircon and apatite fission-track dating of the Early Miocene Patria Quartz Diorite in northwestern Panay indicates rapid cooling at ~12–11 Ma (Walia et al., 2013), and metasedimentary rocks from the Romblon Islands yielded mica K-Ar ages of ~12 Ma (Dimalanta et al., 2009).

Obviously, the thrusting/activity of the Palawan wedge did not cease at the Red Unconformity (13.4–11.5 Ma). It might occur underneath the wedge in the manner of tectonic underplating. Although the thrusting in the external part of the wedge might be weakened, it continued in places as indicated by the syn-thrust sequence (Ilao et al., 2018). Instead, the cessation of thrusting and the pause in uplift of the wedge might occur at the base of the condensed Tabon Limestone (Alfonso XIII Formation) at ~9 Ma, when terrigenous input was suddenly reduced. This timing is consistent with the end of rapid cooling of the Kapoas Granite in northern Palawan at ~8.5±0.4 Ma. In a wider area, the onset of development of the Isugod Basin (13.4–11.5 Ma) and cessation of wedge activity (~9 Ma) in Palawan were roughly correlated with the onset of development of minibasins (13.5–12.5 Ma) and cessation of wedge activity (~10.5 Ma) in northern Borneo (Morley et al., 2023).

It is clear that once the seafloor spreading of the SCS stopped at 16–15 Ma, compression from the southeastward drifting Palawan microcontinental block driven by the ridge push from the SCS spreading would disappear in the arc-continent collision zone in Palawan (Figure 11d). However, arc-continent collision did not stopped at that time and could be last to ~9 Ma as we discussed above. It then requires compression from the Cagayan Ridge on the upper plate to sustain the convergence after 16–15 Ma. Advokaat et al. (2018) and Lai et al. (2020) proposed a ~10° counterclockwise rotation of Borneo since the Early Miocene driven by the Late Oligocene–Early Miocene collision of Sula Spur promontory of the Australian Plate with eastern Sundaland. This rotation might contribute to the motion of the Cagayan Ridge but it would be limited after the Middle Miocene. Alternatively, the compression might be derived from the northward migration of the Luzon Island (being part of the now Philippine Mobile Belt, Figure 1a) which also experienced significant counterclockwise rotation between the Early Miocene and ~10 Ma (Fuller et al. 1991). The Luzon Island located to the northeast to the Cagayan Ridge on the upper plate during the Proto-SCS subduction (Hall, 2012; Lai et al., 2020). It is possible that the Cagayan Ridge had not been decoupled from the Luzon Island after the cessation of the SCS spreading at 16–15 Ma (Figure 11e). Although Hsu et al. (1991) claimed that the Cagayan Ridge had not been rotated or north-south migrated, and thus had been decoupled from the Luzon Island since the middle Miocene, based on the paleomagnetic study on the ODP Site 769 sediments on the southeastern flank of the Cagayan Ridge. However, what they could conclude was only that the Cagayan Ridge had been not been significantly rotated or latitudinally migrated since the Chron C4a/C5 boundary (9.75 Ma), owing to the very poor paleomagnetic data and age-constraint before then.

The sedimentary records from the Isugod Basin allow us to propose a revised model for arc-continent collision in Palawan. As inferred from the age of the metamorphic sole of the Central Palawan Ophiolite (Keenan et al., 2016), the southward subduction of the Proto-SCS initiated at ~34 Ma and was almost simultaneous with the initial spreading of the SCS. However, subduction initiation of the Proto-SCS seems to be diachronous, considering that this event below northern Borneo was proposed to occur at 40–37 Ma as recorded by the Sarawak Orogeny (Advokaat et al., 2018). The subduction of the Proto-SCS generated the Cagayan Ridge volcanic arc on today's Sulu Sea (Figure 12a). An orogenic wedge only developed when the passive continental margin with its thick sediments approached the trench. In response to the arc-continent collision, the Middle Eocene–Early Miocene passive continental margin sequences, primarily the Panas-Pandian (Pulute) Formation were deformed and imbricated into the Palawan wedge through frontal accretion. Foreland flexural subsidence loaded by the orogenic wedge led to the drowning of the Nido carbonate platform and introduction of the basinal Pagasa Formation at ~18 Ma (Steuer et al., 2013), which marks the onset of arc-continent collision (Figure 12b). The onset of collision was also marked by obduction of the forearc ophiolite onto the Palawan continental margin resulted from the underthrusting of the distal Palawan continental margin beneath the NW Sulu Sea (Figure 12b). The shale-prone Pagasa Formation might mainly be derived from the landmass in northern Borneo, with contribution from the embryonic Palawan wedge through submarine erosion. As the collision proceeded, the Pagasa Formation was also incorporated into the front of the orogenic wedge (Figure 12c). A significant uplift pulse in the hinterland of the Palawan wedge initiated at 13.4–11.5 Ma (as marked by the Red Unconformity) and might be primarily triggered by the underplating of the Upper Cretaceous Barton Group on the underside of the wedge (Figure 12c). Meanwhile, oversteepening of the wedge taper resulted in local gravitational collapse of the wedge and the subsidence and formation of the Isugod Basin. The gravitational collapse of the external part of the wedge might be also induced by the unstable, overpressure mudstone of the Pagasa Formation. This uplifting finally led to subaerial exposure of the sedimentary cover of the Palawan wedge (Panas-Pandian Formation) and the obducted forearc ophiolite (Central Palawan Ophiolite) at ~11.5 Ma (Figure 12d). Sediments eroded from the Panas-Pandian Formation and the Central Palawan Ophiolite were thus supplied to the Isugod Basin (Isugod Formation), and they were also supplied to the topographic low on the external part of the wedge (lower Matinloc Formation), forming the Red Unconformity (Figure 12d).

6. Conclusion

We present a comprehensive biostratigraphic and provenance study of the syn-collisional sedimentary rocks of the Isugod Basin in central-southern Palawan and provide insight for the evolution of arc-continent collision between the Palawan microcontinental block and the Cagayan Ridge. Biostratigraphic results integrating planktonic foraminifera and calcareous nannofossils show that the Isugod and Alfonso XIII Formations in the Isugod Basin were deposited in the Late Miocene (11.5–5.6 Ma). These deposits are correlatives to the Matinloc Formation that unconformably overlies the Palawan wedge offshore. Benthic foraminifera from the Isugod Formation indicate rapid tectonic subsidence (>500 m) between the basal limestone and the overlying turbidities, probably resulting from local gravitational collapse of the wedge in response to forearc uplift. Trace elements, Nd isotope data, heavy mineral assemblages and detrital zircon U-Pb geochronology indicates that the siliciclastic sedimentary rocks of the Isugod and the Alfonso

XIII Formations were derived from erosion of both the Panas-Pandian Formation which is the sedimentary cover of the Palawan wedge and the Central Palawan Ophiolite which was part of the forearc basement of the Cagayan Ridge. The Palawan wedge and the obducted ophiolite were uplifted and exposed subaerially by ~11.5 Ma and implies the initiation of arc-continent collision before ~11.5 Ma. However, the collision initiation in Palawan could be better constrained to ~18 Ma, based on the drowning of the Nido carbonate platform in the foreland in response to the flexural subsidence driven by thrust-sheet loading in the Palawan wedge. Therefore, the gravitational collapse of the Palawan wedge and the subsidence/formation of the Isugod Basin might reflect a significant uplift pulse in the hinterland of the wedge beginning within 13.4–11.5 Ma in the late stage of collision, which was also marked by the Red Unconformity offshore Palawan. The uplift pulse in the hinterland of the wedge was probably driven by large-scale underplating of continental rocks beneath the wedge. Although the spreading of the SCS (i.e. the southeastward drifting of the Palawan microcontinetal block) had already ceased at that time, the convergence in the collision zone could be sustained by the counterclockwise rotation of Borneo or the northward migration of Luzon Island on the upper plate.

Acknowledgements

This research was financially supported by the National Key Research and Development Program of China (2023YFF0803403), National Natural Science Foundation of China (grants 41606068, 42076053), Guangzhou Basic and Applied Basic Research Foundation (2023A04J1514), and Early Career Research Program of the State Key Laboratory of Isotope Geochemistry （SKLaBIG-QD-22-03). This is contribution No. xxxx from GIGCAS. We thank Pacle Nichole Anthony D., Villaplaza Barbie Ross B. and Tian Zhixian for their assistance in the fieldwork. We appreciate Sun Shengling, Wu Dan and Yao Deng for their help on the analyses in GIGCAS laboratories. We are also grateful to Yu Mengming for constructive discussions. We are grateful to the editors, the reviewer Dr. Morley Chris, Dr. Licheng Caoand an anonymous reviewer for their valuable and constructive comments which have substantially improved the paper.

Open Research

Data Availability Statement

All the data used in this paper, including micropaleontology, geochemistry, heavy minerals and detrital zircon geochronology data, are provided in Supporting Information and can be also found in Mendeley Data (https://doi.org/10.17632/s863smpdzk.2; Chen et al., 2024).

Reference

Abbott, L. D., Silver, E. A., & Galewsky, J. (1994). Structural evolution of a modern arc-continent collision in Papua New Guinea. *Tectonics*, *13*, 1007–1034. https://doi.org/10.1029/94TC01623

Advokaat, E. L., Marshall, N. T., Li, S., Spakman, W., Krijgsman, W., & van Hinsbergen, D. J. J. (2018). Cenozoic rotation history of Borneo and Sundaland, SE Asia revealed by paleomagnetism, seismic tomography, and kinematic reconstruction. *Tectonics*, *37*(8), 2486–2512. https://doi.org/10.1029/2018TC005010

Anthonissen, D. E., & Ogg J. G. (2012). Appendix 3—Cenozoic and Cretaceous biochronology of planktonic foraminifera and calcareous nannofossil. In F. M. Gradstein et al. (Eds.), *The Geologic Time Scale 2012* (pp. 1083–1127). Boston: Elsevier.

Aurelio, M. A., Forbes, M. T., Taguibao, K. J. L., Savella, R. B., Bacud, J. A., Franke, D., Pubellier M., Savva D., Meresse F., Steuer, S., & Carranza, C. D. (2014). Middle to Late Cenozoic tectonic events in south and central Palawan (Philippines) and their implications to the evolution of the south-eastern margin of South China Sea: Evidence from onshore structural and offshore seismic data. *Marine and Petroleum Geology*, *58,* 658–673. https://doi.org/10.1016/j.marpetgeo.2013.12.002

Aurelio, M.A., & Peña, R.E. (Eds.). (2010). *Geology of the Philippines tectonics and stratigraphy,* (Second ed., Vol. 1.). Quezon City, Philippines: Mines and Geosciences Bureau, Department of Environment and Natural Resources.

Aurelio, M. A., Peña, R. E., & Taguibao, K. J. L. (2013). Sculpting the Philippine archipelago since the Cretaceous through rifting, oceanic spreading, subduction, obduction, collision and strike-slip faulting: Contribution to IGMA5000. *Journal of Asian Earth Sciences, 72*, 102-107.

Bellon, H., & Rangin, C. (1991). Geochemistry and isotopic dating of Cenozoic volcanic arc sequences around the Celebes and Sulu Seas. In E. A. Silver, C. Rangin, M. T. von Breymann, et al., *Proceedings of the Ocean Drilling Program, Scientific Results* (Vol. 124, pp. 321–338). Ocean Drilling Program.

Blow, W. H. (1969). Late Middle Eocene to Recent planktonic foraminiferal biostratigraphy.

In P. Brönnimann & H. H. Renz (Eds.), *Proceedings of the First International Conference on Planktonic Microfossils* (Vol. 1, pp. 199–422). Leiden: E.J. Brill.

Briais, A., Patriat, P., & Tapponnier, P. (1993). Updated interpretation of magnetic anomalies and seafloor spreading stages in the South China Sea: Implications for the Tertiary tectonics of Southeast Asia. *Journal of Geophysical Research: Solid Earth*, *98*(B4), 6299–6328. https://doi.org/10.1029/92JB02280

Boudaugher-Fadel, M. K. (2018). *Evolution and geological significance of larger benthic foraminifer*. (Second ed.). London: UCL Press.

Bouma, A. H. (1962). *Sedimentology of some flysch deposits: A graphic approach to facies interpretation*. Amsterdam: Elsevier Pub.

Burton-Johnson, A., Macpherson, C. G., Millar, I. L., Whitehouse, M. J., Ottley, C. J., & Nowell, G. M. (2020). A Triassic to Jurassic arc in north Borneo: Geochronology, geochemistry, and genesis of the Segama Valley Felsic Intrusions and the Sabah ophiolite. *Gondwana Research, 84,* 229-244.

Cadenas, P., & Ranero, C. R. (2024). Structure and tectonic evolution of the NW Sulu Sea Basin (SE Asia). *Journal of Geophysical Research: Solid Earth*, 129, e2022JB026180. https://doi.org/10.1029/2022JB026180

Cao, L., Shao, L., Qiao, P., Cui, Y., Zhang, G., & Zhang, X. (2021). Formation and paleogeographic evolution of the Palawan continental terrane along the Southeast Asian margin revealed by detrital fingerprints. *Geological Society of America Bulletin*, *133*(5–6), 1167–1193.

Chapman, J. B., & DeCelles, P. G. (2015). Foreland basin stratigraphic control on thrust belt evolution. *Geology*, *43*(7), 579-582.

Chen, W. H., Huang, C. Y., Yan, Y., Dilek, Y., Chen, D., Wang, M. H., et al. (2017). Stratigraphy and provenance of forearc sequences in the Lichi Mélange, Coastal Range: Geological records of the active Taiwan arc-continent collision. *Journal of Geophysical Research: Solid Earth*, *122*(9), 7408–7436. https://doi.org/10.1002/2017JB014378

Chen, W. H., Yan, Y., Carter, A., Clift, P., Huang, C. Y., Yumul Jr., G. P., et al. (2024). Data for Evolution of arc-continent collision in the southeastern margin of the South China Sea: Insight from the Isugod Basin in central-southern Palawan (Version 2) [Dataset]. Mendeley Data. https://doi.org/10.17632/s863smpdzk.2

Chen, W. H., Yan, Y., Carter, A., Huang, C. Y., Yumul Jr., G. P., Dimalanta, C. B., et al. (2021). Stratigraphy and provenance of the Paleogene syn-rift sediments in central-southern Palawan: Paleogeographic significance for the South China Margin. *Tectonics*, *40*(9), e2021TC006753. https://doi.org/10.1029/2021TC006753

Chien, Y. H., Wang, K. L., Chung, S. L., Ghani, A. A., Iizuka, Y., Li, X. H., et al. (2019). Age and genesis of Sabah Ophiolite complexes in NE Borneo. In: Goldschmidt Abstracts, vol. 598.

Clement, J. F., & Keij, J. (1958). Geology of the Kudat Peninsula, North Borneo (Compilation). Annual Report of the Geological Survey Department, GR783.

Clift, P. D., Schouten, H., & Draut, A. E., 2003. A general model of arc-continent collision and subduction polarity reversal from Taiwan and the Irish Caledonides. In R. D. Larter,

& P. T. Leat (Eds.), *Intra-Oceanic Subduction Systems: Tectonic and Magmatic Processes, Geological Society, London, Special Publication* (Vol. 219, pp. 81–98).

Clift, P., & Vannucchi, P. (2004). Controls on tectonic accretion versus erosion in subduction zones: Implications for the origin and recycling of the continental crust. *Reviews of Geophysics*, *42*(2).

Corrado, S., Aldega, L., Perri, F., Critelli, S., Muto, F., Schito, A., & Tripodi, V. (2019). Detecting syn-orogenic extension and sediment provenance of the Cilento wedge top basin (southern Apennines, Italy): Mineralogy and geochemistry of fine-grained sediments and petrography of dispersed organic matter. *Tectonophysics*, *750*, 404–418.

Dewey, J. F. (1988). Extensional collapse of orogens. *Tectonics*, *7*(6), 1123–1139.

Dimalanta, C. B., Ramos, E. G. L., Yumul Jr, G. P., & Bellon, H. (2009). New features from the Romblon Island Group: Key to understanding the arc–continent collision in Central Philippines. *Tectonophysics*, *479*(1–2), 120–129.

Draut, A. E., & Clift, P. D. (2011). Basins in arc-continent collisions. In C. Bushy & A. Azor (Eds.) *Tectonics of sedimentary basins: Recent advances* (pp. 347–368). Hoboken, NJ: Blackwell Publishing Ltd.

Duffy, B., Kalansky, J., Bassett, K., Harris, R., Quigley, M., van Hinsbergen, D. J., et al. (2017). Mélange versus forearc contributions to sedimentation and uplift, during rapid denudation of a young Banda forearc-continent collisional belt. *Journal of Asian Earth Sciences*, *138*, 186–210.

Dycoco, J. M. A., Payot, B. D., Valera, G. T. V., Labis, F. A. C., Pasco, J. A., Perez, A. D., &

Tani, K. (2021). Juxtaposition of Cenozoic and Mesozoic ophiolites in Palawan island, Philippines: New insights on the evolution of the Proto-South China Sea. *Tectonophysics*, *819*, 229085.

Encarnación, J. P., Essene, E. J., Mukasa, S. B., & Hall, C. H. (1995). High-pressure and-temperature subophiolitic kyanite—Garnet amphibolites generated during initiation of mid-Tertiary subduction, Palawan, Philippines. *Journal of Petrology*, *36*(6), 1481–1503.

Forster, M. A., Armstrong, R., Kohn, B., Lister, G. S., Cottam, M. A., & Suggate, S. (2015). Highly retentive core domains in K-feldspar and their implications for ^{40}Ar/^{39}Ar thermochronology illustrated by determining the cooling curve for the Capoas Granite, Palawan, The Philippines. *Australian Journal of Earth Sciences*, *62*(7), 883–902.

Franke, D., Barckhausen, U., Baristeas, N., Engels, M., Ladage, S., Lutz, R., et al. (2011). The continent–ocean transition at the southeastern margin of the South China Sea. *Marine and Petroleum Geology*, *28*(6), 1187–1204. https://doi.org/10.1016/j.marpetgeo.2011.01.004

Fuller, M., Haston, R., Lin, J.-L., Richter, B., Schmidtke, E., & Almasco, J. (1991). Tertiary paleomagnetism of regions around the South China Sea. *Journal of Southeast Asian Earth Sciences*, *6*(3), 161–184. https://doi.org/10.1016/0743-9547(91)90065-6

Gabo, J. A. S., Dimalanta, C. B., Asio, M. G. S., Queaño, K. L., Yumul Jr, G. P., & Imai, A. (2009). Geology and geochemistry of the clastic sequences from Northwestern Panay (Philippines): Implications for provenance and geotectonic setting. *Tectonophysics*, *479*(1–2), 111–119.

Gibaga, C. R. L., Arcilla, C. A., & Hoang, N. (2020). Volcanic rocks from the Central and Southern Palawan Ophiolites, Philippines: Tectonic and mantle heterogeneity constraints. *Journal of Asian Earth Sciences: X*, *4*, 100038.

Hall, R. (2012). Late Jurassic–Cenozoic reconstructions of the Indonesian region and the Indian Ocean. *Tectonophysics*, *570*, 1–41. https://doi.org/10.1016/j.tecto.2012.04.021

Hall, R. (2013). Contraction and extension in northern Borneo driven by subduction rollback. *Journal of Asian Earth Sciences*, *76*, 399–411. https://doi.org/10.1016/j.jseaes.2013.04.010

Harris, R. O. N. (2003). Geodynamic patterns of ophiolites and marginal basins in the Indonesian and New Guinea regions. *Geological Society, London, Special Publications*, *218*(1), 481–505.

Harris, R. (2006). Rise and fall of the Eastern Great Indonesian arc recorded by the assembly, dispersion and accretion of the Banda Terrane, Timor. *Gondwana Research*, *10*(3–4), 207–231.

Harris, R. (2011). The nature of the Banda Arc–continent collision in the Timor region. In D. Brown & P. D. Ryan (Eds.), *Arc-continent collision, Frontiers in Earth Science* (pp. 163–211). Berlin, Heidelberg: Springer.

Harris, R. A., Sawyer, R. K., & Audley-Charles, M. G. (1998). Collisional melange development: Geologic associations of active melange-forming processes with exhumed melange facies in the western Banda orogen, Indonesia. *Tectonics*, *17*(3), 458-479.

Hinz, K. & Schlüter, H. U. (1985). Geology of the Dangerous Grounds, South China Sea, and the continental margin of southwest Palawan: Results of Sonne cruises SO-23 and SO-27. *Energy*, *10*(3–4), 297–315. https://doi.org/10.1016/0360-5442(85)90048-9

Holbourn, A. E., Henderson, A. S., MacLeod, N., & MacLeod, N. (2013). *Atlas of Benthic Foraminifera*. London: Wiley-Blackwell.

Holloway, N. H. (1982). North Palawan block, Philippines–its relation to Asian mainland and role in evolution of South China Sea. *AAPG Bulletin*, *66*, 1355–1383. https://doi.org/10.1306/03B5A7A5-16D1-11D7-8645000102C1865D

Hsu, V. (1991). Paleomagnetic study of deep sea sediments from the Cagayan Ridge in the Sulu Sea: Results of Leg 124. In *Proceedings of the Ocean Drilling Program, Scientific Results* (Vol. 124, pp. 511-516).

Hutchison, C. S., Bergman, S. C., Swauger, D. A., & Graves, J. E. (2000). A Miocene collisional belt in north Borneo: uplift mechanism and isostatic adjustment quantified by thermochronology. *Journal of the Geological Society, London*, *157*, 783–793.

Huang, C. Y., Yuan, P. B., & Tsao, S. J. (2006). Temporal and spatial records of active arc-continent in Taiwan: a synthesis. *Geological Society of America Bulletin*, *118*, 274–288.

Ilao, K. A., Morley, C. K., & Aurelio, M. A. (2018). 3D seismic investigation of the structural and stratigraphic characteristics of the Pagasa Wedge, Southwest Palawan Basin, Philippines, and their tectonic implications. *Journal of Asian Earth Sciences*, *154*, 213–237. https://doi.org/10.1016/j.jseaes.2017.12.017

Jagoutz, O., Macdonald, F. A., & Royden, L. (2016). Low-latitude arc-continent collision as a driver for global cooling. *Proceedings of the National Academy of Sciences. 113*, 4935–4940.

Keenan, T. E. (2016). *Rapid conversion from spreading to subduction: Structural, geochemical, and geochronological studies in Palawan, Philippines* (Doctoral dissertation). Retrieved from ProQuest. (Number 10251558). St. Louis: Saint Louis University.

Keenan, T. E., Encarnación, J., Buchwaldt, R., Fernandez, D., Mattinson, J., Rasoazanamparany, C., & Luetkemeyer, P. B. (2016). Rapid conversion of an oceanic spreading center to a subduction zone inferred from high-precision geochronology. *Proceedings of the National Academy of Sciences*, *113*(47), E7359–E7366. https://doi.org/10.1073/pnas.1609999113

Kudrass, H. R., Muller P., Kreuzer, H., & Weiss, W. (1990). Volcanic rocks and tertiary carbonates dredged from the Cagayan Ridge and the Southwest Sulu Sea, Philippines. In C. Rangin, E. A. Silver, M. T. von Breymann, et al., *Proceedings of the Ocean Drilling Program, Initial Reports*. (Vol. 124, pp. 93–100). College Station, TX: Ocean Drilling Program.

Lai, C. K., Xia, X. P., Hall, R., Meffre, S., Tsikouras, B., Rosana Balangue-Tarriela, M. I., et al. (2020). Cenozoic evolution of the Sulu Sea arc-basin system: An overview. *Tectonics*, e2020TC006630. https://doi.org/10.1029/2020TC006630

Li, C. F., Xu, X., Lin, J., Sun, Z., Zhu, J., Yao, Y.J., et al. (2014). Ages and magnetic structures of the South China Sea constrained by deep tow magnetic surveys and IODP Expedition 349. *Geochemistry, Geophysics, Geosystems, 15,* 4958–4983. https://doi.org/10.1002/ 2014GC005567

Liu, W. N., Li, C. F., Li, J., Fairhead, D., & Zhou, Z. (2014). Deep structures of the Palawan and Sulu Sea and their implications for opening of the South China Sea. *Marine and Petroleum Geology*, 58, 721–735. https://doi.org/10.1016/j.marpetgeo.2014.06.00.5

Lowe, D. R. (1979). Sediment gravity flows: their classification and some problems of application to natural flows and deposits. In *Geology of continental slopes* (Vol. 27, pp. 75-82). SEPM Special publication.

Luan, X., & Lunt, P. (2022). A history of the latest and Neogene unconformities, offshore Palawan and the southern South China Sea. *Journal of Asian Earth Sciences: X*, *8*, 100116.

Lunt, P. (2022). Re-examination of the Base Miocene Unconformity in west Sabah, Malaysia, and stratigraphic evidence against a slab-pull subduction model. *Journal of Asian Earth Sciences*, *230*, 105193.

Lunt, P., & Madon, M. (2017). Onshore to offshore correlation of northern Borneo: a regional perspective. *Bulletin of the Geological Society of Malaysia*, *64*, 101–122.

Macdonald F. A., Swanson-Hysell N. L., Park Y., Lisiecki L., & Jagoutz O. (2019). Arc-continent collisions in the tropics set Earth’s climate state. *Science*, *364*, 181–184.

Malavieille, J., Dominguez, S., Lu, C. Y., Chen, C. T., & Konstantinovskaya, E. (2021). Deformation partitioning in mountain belts: insights from analogue modelling experiments and the Taiwan collisional orogen. *Geological Magazine*, *158*(1), 84–103. https://doi.org/ 10.1017/S0016756819000645

Marchadier, Y. & Rangin, C. (1990). Polyphase tectonics at the southern tip of the Manila trench, Mindoro-Tablas Islands, Philippines. *Tectonophysics*, 183, 273–287.

Martini, E. (1971). Standard Tertiary and Quaternary calcareous nanoplankton zonation. In A. Farinacci (Eds.), *Proceedings of the 2nd International Conference on Planktonic Microfossils* (Vol. 2., pp. 739–785). Roma: Tecnosci.

Miller, K. G., Browning, J.V., Schmelz, W. J., Kopp, R. E., Mountain, G. S., & Wright, J.D., 2020. Cenozoic sea-level and cryospheric evolution from deep-sea geochemical and continental margin records. *Science Advances*, *6*(20), eaaz1346. https://doi.org/10.1126/sciadv.aaz1346.

Mitchell, A. H. G., Hernandez, F. T., & Dela Cruz, A. P. (1986). Cenozoic evolution of the Philippine Archipelago. *Journal of Southeast Asian Earth Sciences*, *1*(1), 3–22.

Morley C. K. (2016). Major unconformities/termination of extension events and associated surfaces in the South China Seas: review and implications for tectonic development. *Journal of Asian Earth Sciences*, *120*, 62–86. https://doi.org/10.1016/j.jseaes.2016.01.013.

Morley, C. K. (2024). Atypical syn-collisional wedges at thrust fronts: Their tectonic and gravity-driven development, and interpretation-related controversies. *Earth-Science Reviews*, 104663.

Morley, C. K., Promrak, W., Apuanram, W., Chaiyo, P., Chantraprasert, S., Ong, D., Suphawajruksakul, A., Thaemsiri, N., & Tingay, M. (2023). A major Miocene deepwater mud canopy system: The North Sabah–Pagasa Wedge, northwestern Borneo. *Geosphere*, *19*(1), 291-334.

Murray, J. W. (1991). *Ecology and Paleoecology of Benthic Foraminifera*. Harlow, Essex, UK: Longman Scientific and Technical.

Omang, S. A., & Barber, A. J. (1996). Origin and tectonic significance of the metamorphic rocks associated with the Darvel Bay Ophiolite, Sabah, Malaysia. *Geological Society, London*, *Special Publications*, *106*(1), 263-279.

Padrones, J. T., Tani, K., Tsutsumi, Y., & Imai, A. (2017). Imprints of Late Mesozoic tectono-magmatic events on Palawan Continental Block in northern Palawan, Philippines. *Journal of Asian Earth Sciences*, *142*, 56–76. http://dx.doi.org/10.1016/j.jseaes.2017.01.027

Parkinson, C. D., Miyazaki, K., Wakita, K., Barber, A. J., & Carswell, D. A. (1998). An overview and tectonic synthesis of the pre-Tertiary very-high-pressure metamorphic and associated rocks of Java, Sulawesi and Kalimantan, Indonesia. *Island Arc*, *7*(1–2), 184–200.

Platt, J. P., & Vissers, R .L. M. (1989). Extensional collapse of thickened continental lithosphere: A working hypothesis for the Alboran Sea and Gibraltar Arc. *Geology*, *17*, 540–543.

Platt, J. P. (1986). Dynamics of orogenic wedges and the uplift of high-pressure metamorphic rocks. *Geological Society of America Bulletin*, *97*(9), 1037–1053.

Rahim, A. R., Konjing, Z., Asis, J., Nursyazwani, A. J., Muhamad, A. J., Ibrahim, N., et al. (2017). Tectonostratigraphic terranes of Kudat Peninsula, Sabah. *Bulletin of the Geological Society of Malaysia*, *64*, 123–139.

Rangin, C., & Silver, E. A. (1991). Neogene tectonic evolution of the Celebes-Sulu basins: new insights from Leg 124 drilling. In E. A. Silver, C. Rangin, M. T. von Breymann, et al., *Proceedings of the Ocean Drilling Program, Scientific Results* (Vol. 124, pp. 51–63). Ocean Drilling Program. https://doi.org/10.2973/odp.proc.sr.124.122.1991

Rehm, S. (2002). The Miocene Carbonates in Time and Space On- and Offshore SW Palawan, Philippines. Kiel: Mathematisch-Naturwissenschaftliche Fakultät. Christian-Albrechts-University.

Rolland, Y., Hässig, M., Bosch, D., Bruguier, O., Melis, R., Galoyan, G., et al. (2020). The East Anatolia–Lesser Caucasus ophiolite: An exceptional case of large-scale obduction, synthesis of data and numerical modelling. *Geoscience Frontiers*, *11*(1), 83–108.

Royden, L. H. (1993). Evolution of retreating subduction boundaries formed during continental collision. *Tectonics*, *12*(3), 629–638. https://doi.org/0278-7407/93/92TC-02641

Rubatto, D., & Gebauer, D. (2000). Use of cathodoluminescence for U-Pb zircon dating by ion microprobe: some examples from the Western Alps. In M. Pagel (Eds.), *Cathodoluminescence in geosciences* (pp. 373-400). Berlin Heidelberg: Springer-Verlag.

Rudnick, R. L. (1995). Making continental crust. *Nature*, *378*, 571–578.

Rudnick, R. L., & Gao, S. (2003). Composition of the continental crust. In R. L. Rudnick, (Eds.), Treatise on Geochemistry, vol. 3, The Crust (Vol. 3, pp. 1–64). New York: Elsevier.

Ruh, J. B. (2017). Effect of fluid pressure distribution on the structural evolution of accretionary wedges. *Terra Nova*, *29*(3), 202–210. https://doi.org/10.1111/ter.12263

Ruh, J. B. (2020). Numerical modeling of tectonic underplating in accretionary wedge systems. *Geosphere*, *16*(6), 1385–1407. https://doi.org /10.1130 /GES02273.1

Ryan, P. D., & Dewey, J. F. (2019). The Ordovician Grampian Orogeny, western Ireland: Obduction versus "bulldozing" during arc-continent collision. *Tectonics*, *38*, 3462–3475. https://doi.org/10.1029/2019TC005602

Sales, A. O., Jacobsen, E. C., Morado Jr, A. A., Benavidez, J. J., Navarro, F. A., & Lim, A. E. (1997). The petroleum potential of deep-water northwestPalawan Block GSEC 66. *Journal of Asian Earth Sciences*, *15*(2-3), 217-240.

Savva, D., Pubellier, M., Franke, D., Chamot-Rooke, N., Meresse, F., Steuer, S., & Auxietre, J. L. (2014). Different expressions of rifting on the South China Sea margins. *Marine and Petroleum Geology*, *58*, 579–598.

Shao, L., Cao, L., Qiao, P., Zhang, X., Li, Q., & van Hinsbergen, D. J. (2017). Cretaceous–Eocene provenance connections between the Palawan Continental Terrane and the northern South China Sea margin. *Earth and Planetary Science Letters*, *477*, 97–107. https://doi.org/10.1016/j.epsl.2017.08.019

Simoes, M., Avouac, J. P., Beyssac, O., Goffé, B., Farley, K. A., & Chen, Y. G. (2007). Mountain building in Taiwan: A thermokinematic model. *Journal of Geophysical Research: Solid Earth*, *112*(B11). https://doi.org/10.1029/2006JB004824

Steuer, S., Franke, D., Meresse, F., Savva, D., Pubellier, M., Auxietre, J. L., & Aurelio, M. (2013). Time constraints on the evolution of southern Palawan Island, Philippines from onshore and offshore correlation of Miocene limestones. *Journal of Asian Earth Sciences*, *76*, 412–427. https://doi.org/10.1016/j.jseaes.2013.01.007

Steuer, S., Franke, D., Meresse, F., Savva, D., Pubellier, M., & Auxietre, J. L. (2014). Oligocene–Miocene carbonates and their role for constraining the rifting and collision history of the Dangerous Grounds, South China Sea. *Marine and Petroleum Geology*, *58*, 644–657.

Suggate, S. M., Cottam, M. A., Hall, R., Sevastjanova, I., Forster, M. A., White, L. T., et al. (2014). South China continental margin signature for sandstones and granites from Palawan, Philippines. *Gondwana Research*. *26*(2), 699–718. https://doi.org/10.1016/j.gr.2013.07.006.

Suggate, S. M., & Hall, R. (2014). Using detrital garnet compositions to determine provenance: a new compositional database and procedure. *Geological Society, London, Special Publications*, *386*(1), 373-393.

Sun, S. S. & McDonough, W. S. (1989). Chemical and isotopic systematics of oceanic basalts: Implications for mantle composition and processes. *Geological Society, London, Special Publications*, *42*(1), 313–345. https://doi.org/10.1144/GSL.SP.1989.042.01.19

Sutherland, R., Stagpoole, V., Uruski, C., Kennedy, C., Bassett, D., Henrys, S., et al. (2009). Reactivation of tectonics, crustal underplating, and uplift after 60 Myr of passive subsidence, Raukumara Basin, Hikurangi-Kermadec fore arc, New Zealand: Implications for global growth and recycling of continents. *Tectonics*, *28*(5), TC5017. https://doi.org/0278-7407/09/2008TC002356

Smye, A. J., Greenwood, L. V., & Holland, T. J. B. (2010). Garnet–chloritoid–kyanite assemblages: eclogite facies indicators of subduction constraints in orogenic belts. Journal of Metamorphic Geology, 28(7), 753–768.

Suzuki, S., Takemura, S., Yumul, G. P., David, S. D., & Asiedu, D. K. (2000). Composition and provenance of the Upper Cretaceous to Eocene sandstones in Central Palawan, Philippines: Constraints on the tectonic development of Palawan. *Island Arc*, *9*(4), 611–626.

Tate, G. W., McQuarrie, N., van Hinsbergen, D. J. J., Bakker, R. R., Harris, R., Willett, S., et al. (2014). Resolving spatial heterogeneities in exhumation and surface uplift in Timor-Leste: Constraints on deformation processes in young orogens. *Tectonics*, *33*(6), 1089–1112. https://doi.org/10.1002/2013TC003436

Taylor, B., & Hayes, D. E. (1983). Origin and history of the South China Sea basin. In D. E. Hayes, (Eds.), *The Tectonic and Geologic Evolution of Southeast Asian Seas and Islands: Part 2, Geophysical Monograph Series* (Vol. 27, pp. 23–56). Washington, DC: American Geophysical Union. https://doi.org/10.1029/GM027p0023

Tong, D., Ren, J., Liao, Y., Yao, Y., & Zhao, Y. (2019). Cenozoic tectonic events and their implications for constraining the structure and stratigraphic styles from rifting to collision at the southeastern margin of the South China Sea. *Marine Geophysical Research*, *40*, 145–161.

Tongkul, F. (1994). The geology of Northern Sabah, Malaysia: its relationship to the opening of the South China Sea Basin. *Tectonophysics*, *235*(1–2), 131-147.

Tsikouras, B., Lai, C. K., Ifandi, E., Teo, C. H., & Xia, X. P. (2021). New zircon radiometric U-Pb ages and Lu-Hf isotopic data from the ultramafic-mafic sequences of Ranau and Telupid (Sabah, eastern Malaysia): Time to reconsider the geological evolution of Southeast Asia? *Geology*, *49*(7), 789–793.

Underwood, M. B. & Moore, G. F. (1995). Trenches and trench-slope basins. In C. J. Busby, & R. V. Ingersoll, (Eds.), *Tectonics of Sedimentary Basins* (pp. 179–219). Cambridge: Blackwell Scientific.

Valera, G. T. V., Kawakami, T., & Payot, B. D. (2022). The slab–mantle wedge interface of an incipient subduction zone: Insights from the P–T–D evolution and petrological characteristics of the Dalrymple Amphibolite, Palawan Ophiolite, Philippines. *Journal of Metamorphic Geology*, *40*(4), 717–749.

van Hattum, M. W. A. (2005). *Provenance of Cenozoic sedimentary rocks of northern Borneo* (Doctoral dissertation, Royal Holloway, University of London).

van Hattum, M. W. A., Hall, R., Pickard, A. L., & Nichols, G. J. (2013). Provenance and geochronology of Cenozoic sandstones of northern Borneo. *Journal of Asian Earth Sciences*, *76*, 266–282.

Vermeesch, P. (2013). Multi-sample comparison of detrital age distributions. *Chemical Geology*, *341*, 140–146. https://doi.org/10.1016/j.chemgeo.2013.01.010

Wade, B. S., Pearson, P. N., Berggren, W. A., & Palike, H. (2011). Review and revision of Cenozoic tropical planktonic foraminiferal biostratigraphy and calibration to the geomagnetic polarity and astronomical time scale. *Earth-Science Reviews*, *104*(1–3), 111–142. https://doi.org/10.1016/j.earscirev.2010.09.003

Wakabayashi, J., & Dilek, Y. (2003). What constitutes ‘emplacement’of an ophiolite?: Mechanisms and relationship to subduction initiation and formation of metamorphic soles. *Geological Society, London, Special Publications*, *218*(1), 427-447.

Walia, M., Knittel, U., Suzuki, S., Chung, S. L., Pena, R. E., & Yang, T. F. (2012). No Paleozoic metamorphics in Palawan (the Philippines)? Evidence from single grain U-Pb dating of detrital zircons. *Journal of Asian Earth Sciences*, *52*, 134–145. https://doi.org/10.1016/j.jseaes.2012.03.005

Walia, M., Yang, T. F., Knittel, U., Liu, T. K., Lo, C. H., Chung, S. L., et al. (2013). Cenozoic tectonics in the Buruanga Peninsula, Panay Island, Central Philippines, as constrained by U-Pb, ^{40}Ar/^{39}Ar and fission track thermochronometers. *Tectonophysics*, *582*, 205–220.

Wang, Y., Qian, X., Asis, J. B., Cawood, P. A., Wu, S., Zhang, Y., et al. (2023). “Where, when and why” for the arc-trench gap from Mesozoic Paleo-Pacific subduction zone: Sabah Triassic-Cretaceous igneous records in East Borneo. *Gondwana Research*, *117*, 117–138.

Williams, H. H. (1997). Play concepts-northwest Palawan, Philippines. *Journal of Asian Earth Sciences*, *2*(15), 251–273.

Wolfart, R., Čepek, P., Gramann, F., Kemper, E., & Porth, H. (1986). Stratigraphy of Palawan Island, Philippines. *Newsletters on Stratigraphy*, *16*(1), 19–48.

Yan, Y., Yao, D., Tian, Z., Huang, C., Chen, W., Santosh, M., et al. (2018). Zircon U-Pb chronology and Hf isotope from the Palawan-Mindoro Block, Philippines: Implication to provenance and tectonic evolution of the South China Sea. *Tectonics*, *37*(4), 1063–1076. https://doi.org/10.1002/2017TC004942

Yumul Jr., G. P., Dimalanta, C. B., Marquez, E. J., & Queaño, K. L. (2009). Onland signatures of the Palawan microcontinental block and Philippine mobile belt collision and crustal growth process: a review. *Journal of Asian Earth Sciences*, *34*, 610–623. https://doi.org/10.1016/j.jseaes.2008.10.002

Reference From the Supporting Information

Huang, C., Wang, H., Yang, J. H., Ramezani, J., Yang, C., Zhang, S. B., et al. (2020). SA01–A proposed zircon reference material for microbeam U-Pb age and Hf-O isotopic determination. *Geostandards and Geoanalytical Research*, *44*(1), 103–123.

Jacobsen, S. B., & Wasserburg, G. J. (1980). Sm-Nd isotopic evolution of chondrites. *Earth and Planetary Science Letters*, *50*(1), 139–155. https://doi.org/10.1016/0012-821X(80)90125-9

Liu, Y., Hu, Z., Zong, K., Gao, C., Gao, S., Xu, J., & Chen, H. (2010). Reappraisement and refinement of zircon U-Pb isotope and trace element analyses by LA-ICP-MS. *Chinese*

Science Bulletin. *55*, 1535–1546. https://doi.org/10.1007/s11434-010-3052-4

Liu, Y., Liu, H. C., & Li, X. H. (1996). Simultaneous and precise determination of 40 trace elements in rock samples using ICP-MS. *Geochimica*, *25*(6), 552–558 (in Chinese with English abstract).

Ludwig, K. R. (2003). User's manual for isoplot 3.00, a geochronlogical toolkit for Microsoft Excel. *Berkeley Geochronology Central Special Publication*, *4*, 25–32.

Paton, C., Hellstrom, J., Paul, B., Woodhead, J., & Hergt, J. (2011). Iolite: Freeware for the visualisation and processing of mass spectrometric data. *Journal of Analytical Atomic Spectrometry*, *26*(12), 2508–2518.

Sláma, J., Košler, J., Condon, D. J., Crowley, J. L., Gerdes, A., Hanchar, J. M., et al. (2008). Plešovice zircon—a new natural reference material for U-Pb and Hf isotopic microanalysis. *Chemical Geology*, *249*, 1–35. https://doi.org/10.1016/j.chemgeo.2007.11.005van Morkhoven F. P., Berggren, W. A., Edwards, A. S., & Oertli, H. J. (1986). Cenozoic cosmopolitan deep-water benthic foraminifera. In *Bulletin des Centres de Recherches Exploration Production* (Memoire no. 11). Pau: Elf Aquitaine.

Wei, G. J., Liang, X. R., Li, X. H., & Liu, Y. (2002). Precise measurement of Sr isotopic composition of liquid and solid base using (LP)MC-ICPMS. *Geochimica*, *31* (3), 295–299 (in Chinese with English abstract). https://doi.org/10.1080/12265080208422884

Wiedenbeck, M., Hanchar, J. M., Peck, W. H., Sylvester, P., Valley, J., Whitehouse, M., et al. (2004). Further characterisation of the 91500 zircon crystal. *Geostandards and Geoanalytical Research*, *28*(1), 9-39.

https://doi.org/10.1111/j.1751-908X.2004.tb01041.x

Figure Captions (color online only for all figures)

Figure 1. (a) Topographic map of the South China Sea region, showing the boundary of the Palawan microcontinental block (modified from Liu et al., 2014) and the Cagayan Ridge. The white dots in the SE Sulu Sea represent ODP sites. RI= Romblon Islands; PT=Palawan Trough; NWBT= NW Borneo Trough; KF=Kudat Formation. (b) Geological map of Palawan Island simplified from Aurelio & Peña, 2010); CPO=Central Palawan Ophiolite; SPO=Southern Palawan Ophiolite. (c) Geologic map of the Isugod Basin in central-southern Palawan. The sample names in italics denote sandstone samples, while the rest represent mudstone samples. (d) A NW-SW cross section of central-southern Palawan, see the location of section in Figure 1a. Large uncertainties might exist in the imbricate thrusts in the Central Palawan Ophiolite, as inferred from the contact relationship between each unit of the ophiolite mapped in Figure 1b by Aurelio & Peña (2010).

Figure 2. (a) Field photographs of outcrops of the Isugod Formation (a–f) and the Alfonso XIII Formation (g–i). (a) Greyish white massive limestone at the Taraw Cave at Site QU-03 at the base of the Isugod Formation, the inset showing the coral fossil dropped from the limestone. (b) The grey thin-bedded mudstone and very thin-beded sandstone interbeds exposed on the floor of the shallow roadside ditch at Site QU-12. (c) Alternations of greyish green thin-bedded sandstone and dark grey medium-bedded mudstone at Site QU-26. (d) Sandstone bed with parallel and cross bedding at Site QU-26. (e) Dark grey thin-bedded mudstone intercalated with several beds of light grey sandstone at Site QU-22. The thickness of the sandstone beds varies from 5 to 40 cm. (f) Pebbly mudstone at Site QU-13. (g) Light grey thin to medium bedded limestone at Site QU-01. (h) Cream thin-bedded calcareous mudstone. (i) Cream thick bedded calcareous siltstone graded upward into calcareous mudstone.

Figure 3. (a) SEM images of planktonic foraminifera recovered from the Isugod Formation (numbers 1–10) and the Alfonso XIII Formation (numbers 11–20) are shown with scale bars of 200 μm. Numbers (1–6) recovered from Sample QU-12b: (1) *Globorotalia mayeri* Cushman & Ellisor; (2) *Orbulina suturalis* Brönnimann; (3) *Globoquadrina dehiscens* (Chapman, Parr & Collins); (4) *Dentoglobigerina altispira* (Cushman & Jarvis); (5) *Globigerina decoraperta* Takayanagi & Saito; (6) *Groborotalia paralenguaensis* Blow. Numbers (7–9) recovered from Sample QU-13a: (7) *Globorotalia mayeri* Cushman & Ellisor; (8) *Globoquadrina dehiscens* (Chapman, Parr & Collins); (9) *Globigerina nepenthes* Todd. (10) *Globorotalia mayeri* Cushman & Ellisor, recovered from Sample QU-26b. Numbers (11–12) recovered from Sample QU-10c: (11) *Neogloboquadrina acostaensis* (Blow); (12) *Globigerina nepenthes* Todd. (13) *Globigerinoides extremus* Bolli & Bermúdez, recovered from Sample QU-24. Numbers (14–20) recovered from Sample QU-25: (14) *Globigerina nepenthes* Todd; (15) *Neogloboquadrina acostaensis* (Blow); (16) *Globigerina decoraperta* Takayanagi & Saito; (17) *Globigerinoides extremus* Bolli & Bermúdez; (18) *Globorotalia plesiotumida* Blow & Banner; (19) *Globorotalia margaritae* (Bolli & Bermúdez); (20) *Globigerinoides conglobatus* (Brady). **(b)** Polarizing photographs of calcareous nannofossil

recovered from the Isugod Formation (numbers 1–12) and the Alfonso XIII Formation (numbers 13–16) are shown with their approximate diameter of the fossil (red bar). Numbers (1–2) recovered from Sample QU-12b: (1) *Discoaster bollii* Martini & Bramlette; (2) *Discoaster hamatus* Martini & Bramlette. Numbers (3–5) recovered from Sample QU-13a: (3) *Discoaster kugleri* Martini & Bramlette; (4) *Discoaster bollii* Martini & Bramlette; (5) *Reticulofenestra pseudoumbilica* (Gartner). Numbers (6–8) recovered from Sample QU-22b: (6) *Discoaster hamatus* Martini & Bramlette; (7) *Discoaster variabilis* Martini & Bramlette; (8) *Sphenolithus moriformis* Brönnimann & Stradner. Numbers (9–12) recovered from Sample QU-26b: (9–10) *Discoaster kugleri* Martini & Bramlette; (11) *Discoaster exilis* Martini & Bramlette; (12) *Reticulofenestra pseudoumbilica* (Gartner). Numbers (13–16) recovered from Sample QU-10c: (13) *Discoaster hamatus* Martini & Bramlette; (14) *Discoaster bellus* Burky & Percival; (15) *Discoaster asymmetricus* Gartner; (16) *Discoaster braarudii* Bukry.

Figure 4. Datum planes (first appearance datum and last appearance datum) of planktonic foraminifera and calcareous nannofossils (marked by short horizontal bars with numerical age), given according to Wade et al. (2011) and Anthonissen & Ogg (2012), respectively. The age ranges of the Isugod Formation and the Alfonso XIII Formation are enclosed by green and orange rectangles, respectively.

Figure 5. Paleobathymetry of the Isugod Basin, as determined from the benthic foraminiferal assemblage. Bathymetric range of the benthic foraminifera primarily follows Murray (1991) and Holbourn et al. (2013). Also shown are the smoothed global eustatic curve of Miller et al. (2020).

Figure 6. (a) Upper continental crust (UCC) (Rudnick & Gao, 2003) normalized multi-trace element diagram and (b) Chondrite-normalized REE distribution diagram for the Isugod Formation and Alfonso XIII Formation mudstones, as compared with the Isugod Formation sediments published by Cao et al. (2021), the middle Eocene–lowest Oligocene Panas-Pandian sediments (Cao et al., 2021; Chen et al., 2021) and the Upper Cretaceous Barton Group (Cao et al., 2021). The chondrite values are cited from Sun & McDonough (1989).

Figure 7. Heavy mineral assemblage from the Isugod Formation sandstones, as compared with the data published by Cao et al., 2021) and Suggate et al. (2014). The average composition of the heavy mineral from the middle Eocene–lowest Oligocene Panas-Pandian Formation (Cao et al., 2021; Chen et al., 2021; Shao et al., 2017) and the Upper Cretaceous Barton Group (Cao et al., 2021; Shao et al., 2017; Suggate et al., 2014) are also shown.

Figure 8. Comparison of U-Pb age spectra for detrital zircon from (a-e) the Isugod Formation samples of this study (115 detrital zircon U-Pb ages in total from samples QU-26a and QU-27a has been reported earlier in Yan et al., 2018), (f) the Isugod Formation samples published by Cao et al. (2021) and Suggate et al. (2014), (g) the Middle Eocene–earliest Oligocene Panas-Pandian Formation (Chen et al., 2021; Shao et al., 2017; Yan et al., 2018) and (h) the Late Cretaceous Barton Group (Shao et al., 2017; Suggate et al., 2014; Walia et al., 2012). (i) &(j) Nonmetric multidimensional scaling (MDS**)** map (Vermeesch et al., 2013) for detrital zircon U-Pb ages of the Late Cretaceous to Miocene sediments in Palawan, when the two young age groups (13–15 Ma and 30–52.5 Ma) in the Isugod Formation are included (i) or excluded (j). The stress value is 0.077 and 0.074, respectively, indicating good

goodness-of-fits. Solid and dashed lines in the map indicate the closest and second closest neighbors, respectively.

Figure 9. Correlation of offshore and onland stratigraphy of central and southern Palawan. The offshore stratigraphy is mainly after Ilao et al. (2018), Luan & Lunt (2022) and Steuer et al. (2013). Both onland stratigraphy of previous study (Aurelio et al., 2014; Ilao et al., 2018; Wolfart et al., 1986) and this study and are presented. The Middle Eocene–Early Miocene onland stratigraphy of this study is adopted from Chen et al. (2021). RU/MMU=Red Unconformity/Middle Miocene Unconformity.

Figure 10. (a) Plot of Co/Th versus La/Sc and Tertiary plots of (b) La-Th-Sc and (c) Th-Sc-Zr/10 of the Isugod Formation and Alfonso XIII Formation mudstones, as compared with the Isugod Formation sediments published by Cao et al. (2021), the Middle Eocene–lowest Oligocene Panas-Pandian sediments (Cao et al., 2021; Chen et al., 2021) and the Late Cretaceous Barton Group (Cao et al., 2021) and the Palawan ophiolites (Gibaga et al., 2020; Keenan et al., 2016). (d) Simple two-component mixing models based on Nd isotopes for the Isugod Formation and Alfonso XIII Formation. The two end-members are the Panas-Pandian Formation (Nd=40.5 ppm, ε_{Nd}=-8.7 in average) (Chen et al., 2021) and the Palawan Ophiolite (Nd=9.9 ppm, ε_{Nd}=9.4 for the Central Palawan Ophiolite and Nd=4.25 ppm, ε_{Nd}=5.4 for the Southern Palawan Ophiolite, respectively) (Gibaga et al., 2020).

Figure 11. Simple tectonic evolution map of the South China Sea region (modified from Advokaat et al., 2018; Hall, 2012; Lai et al., 2020; Morley, 2024), showing (a) the initiation of the South China Sea spreading accommodated by the southward subduction of the Proto-SCS at ~33 Ma (it is noted that subduction initiation in the segment of Palawan-Cagayan Ridge occurred along or near an Eocene spreading center), (b) the initiation of collision in Sabah (northern Borneo) at ~23 Ma, (c) the initiation of collision in Palawan at ~18 Ma, (d) the cessation of the of the South China Sea spreading at ~15 Ma, and (e) the ongoing arc-continent collision at ~11.5 Ma in Palawan after the cessation of the of the South China Sea spreading.

Figure 12. Proposed tectonic model for the evolution of arc-continent collision in Palawan (modified after Rangin & Silver, 1991). SCS=South China Sea; CPO=Central Palawan Ophiolite; IB=Isugod Basin.

Figure 1.

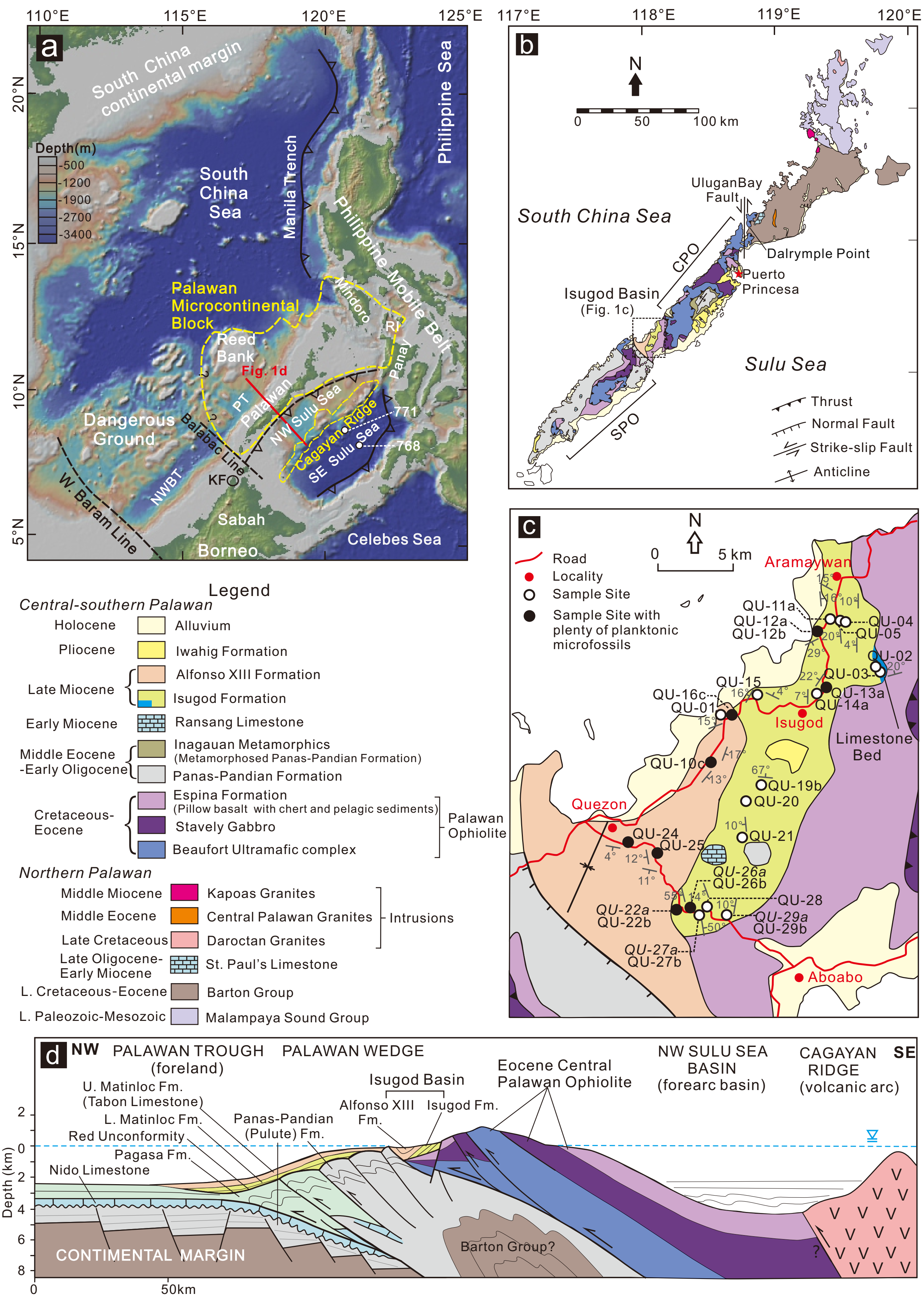

a
South China continental margin
South China Sea
Manila Trench
Philippine Sea
Philippine Mobile Belt
Palawan Microcontinental Block
Reed Bank
Mindoro
Panay
Fig. 1d
PT
Palawan
NW Sulu Sea
Cagayan Ridge
SE Sulu Sea
771
768
Dangerous Ground
Balabac Line
W. Baram Line
NWBT
KF
Sabah
Borneo
Celebes Sea
Depth(m)
b
South China Sea
Sulu Sea
UluganBay Fault
Dalrymple Point
Puerto Princesa
Isugod Basin (Fig. 1c)
CPO
SPO
Thrust
Normal Fault
Strike-slip Fault
Anticline
c
Road
Locality
Sample Site
Sample Site with plenty of planktonic microfossils
Aramaywan
Isugod
Quezon
Aboabo
Limestone Bed
Legend
Central-southern Palawan
Holocene — Alluvium
Pliocene — Iwahig Formation
Late Miocene — Alfonso XIII Formation; Isugod Formation
Early Miocene — Ransang Limestone
Middle Eocene -Early Oligocene — Inagauan Metamorphics (Metamorphosed Panas-Pandian Formation); Panas-Pandian Formation
Cretaceous-Eocene — Espina Formation (Pillow basalt with chert and pelagic sediments); Stavely Gabbro; Beaufort Ultramafic complex — Palawan Ophiolite
Northern Palawan
Middle Miocene — Kapoas Granites
Middle Eocene — Central Palawan Granites
Late Cretaceous — Daroctan Granites — Intrusions
Late Oligocene-Early Miocene — St. Paul's Limestone
L. Cretaceous-Eocene — Barton Group
L. Paleozoic-Mesozoic — Malampaya Sound Group
d
NW
SE
PALAWAN TROUGH (foreland)
PALAWAN WEDGE
Isugod Basin
Eocene Central Palawan Ophiolite
NW SULU SEA BASIN (forearc basin)
CAGAYAN RIDGE (volcanic arc)
U. Matinloc Fm. (Tabon Limestone)
L. Matinloc Fm.
Red Unconformity
Pagasa Fm.
Nido Limestone
Panas-Pandian (Pulute) Fm.
Alfonso XIII Fm.
Isugod Fm.
Barton Group?
CONTIMENTAL MARGIN
Depth (km)
50km

Figure 2.

a
Site QU-03
b
Site QU-12
c
Site QU-26
d
Site QU-26
e
Site QU-22
f
Site QU-13
g
Site QU-01
h
Site QU-24
i
Site QU-25
Isugod Formation
Alfonso XIII Formation

Figure 3.

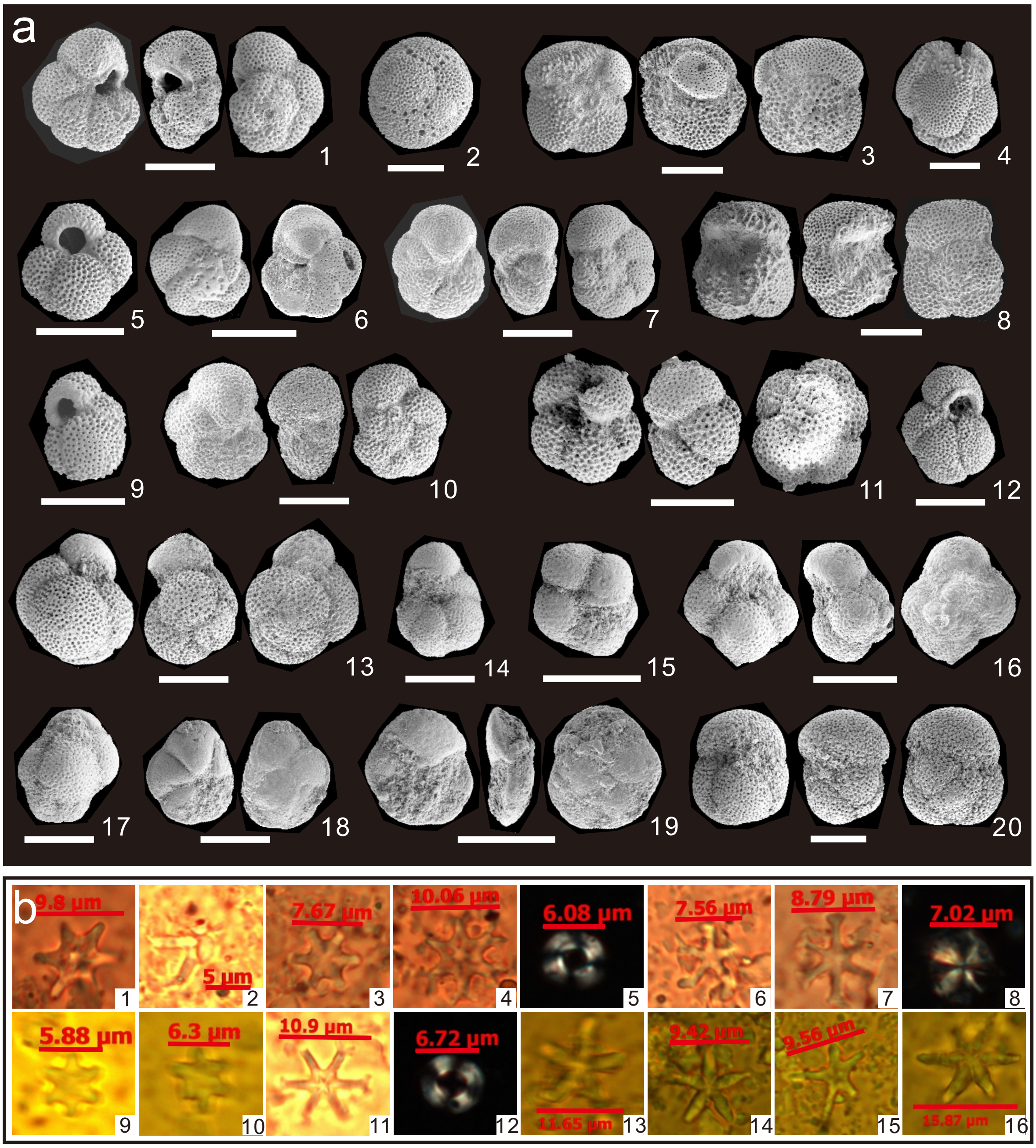
a
1
2
3
4
5
6
7
8
9
10
11
12
13
14
15
16
17
18
19
20
b
9.8 µm
5 µm
7.67 µm
10.06 µm
6.08 µm
7.56 µm
8.79 µm
7.02 µm
5.88 µm
6.3 µm
10.9 µm
6.72 µm
11.65 µm
9.42 µm
9.56 µm
15.87 µm

Figure 4.

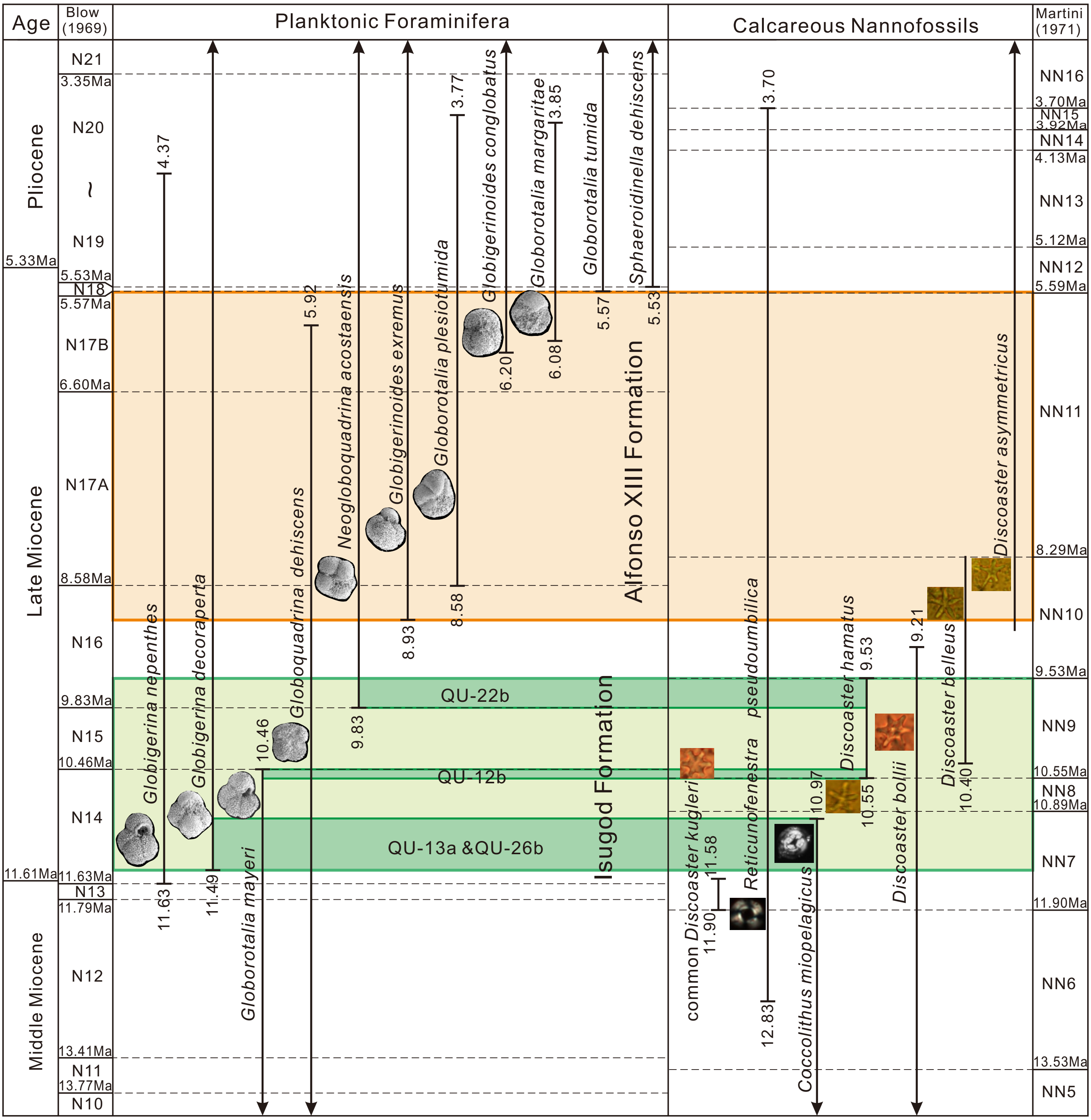

Age
Blow (1969)
Planktonic Foraminifera
Calcareous Nannofossils
Martini (1971)
Pliocene
Late Miocene
Middle Miocene
5.33Ma
11.61Ma
N21
3.35Ma
N20
~
N19
5.53Ma
N18
5.57Ma
N17B
6.60Ma
N17A
8.58Ma
N16
9.83Ma
N15
10.46Ma
N14
11.63Ma
N13
11.79Ma
N12
13.41Ma
N11
13.77Ma
N10
NN16
3.70Ma
NN15
3.92Ma
NN14
4.13Ma
NN13
5.12Ma
NN12
5.59Ma
NN11
8.29Ma
NN10
9.53Ma
NN9
10.55Ma
NN8
10.89Ma
NN7
11.90Ma
NN6
13.53Ma
NN5
Globigerina nepenthes
Globigerina decoraperta
Globorotalia mayeri
Globoquadrina dehiscens
Neogloboquadrina acostaensis
Globigerinoides exremus
Globorotalia plesiotumida
Globigerinoides conglobatus
Globorotalia margaritae
Globorotalia tumida
Sphaeroidinella dehiscens
4.37
11.63
11.49
10.46
5.92
9.83
8.93
3.77
8.58
6.20
3.85
6.08
5.57
5.53
Alfonso XIII Formation
Isugod Formation
QU-22b
QU-12b
QU-13a &QU-26b
common Discoaster kugleri
11.58
11.90
Reticunofenestra pseudoumbilica
3.70
12.83
Coccolithus miopelagicus
10.97
Discoaster hamatus
9.53
10.55
Discoaster bollii
9.21
Discoaster belleus
10.40
Discoaster asymmetricus

Figure 5.

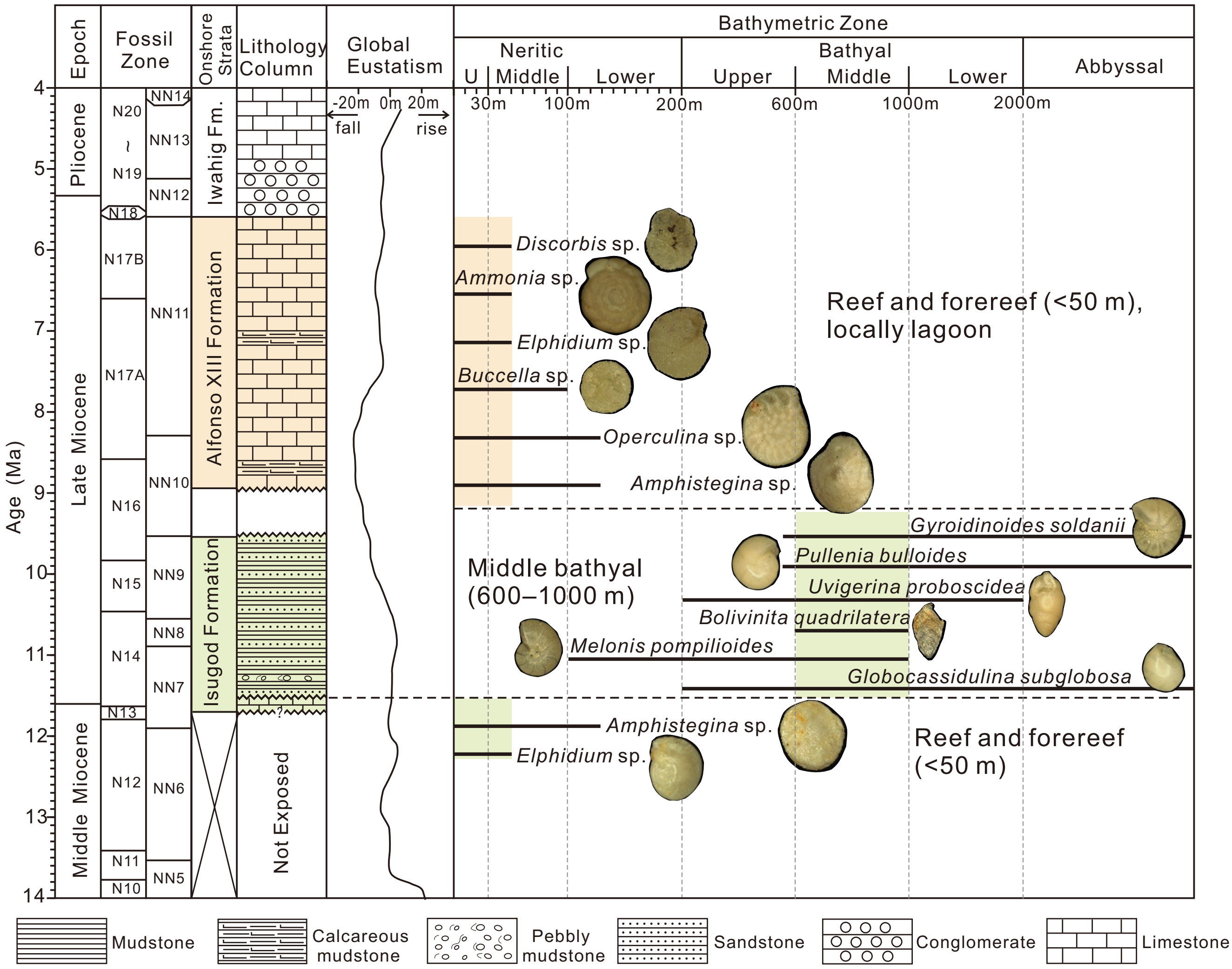
Epoch
Fossil Zone
Onshore Strata
Lithology Column
Global Eustatism
Bathymetric Zone
Neritic
U
Middle
Lower
Bathyal
Upper
Middle
Lower
Abbyssal
Age (Ma)
-20m
0m
20m
fall
rise
30m
100m
200m
600m
1000m
2000m
Pliocene
Late Miocene
Middle Miocene
N20
N19
N18
N17B
N17A
N16
N15
N14
N13
N12
N11
N10
NN14
NN13
NN12
NN11
NN10
NN9
NN8
NN7
NN6
NN5
Iwahig Fm.
Alfonso XIII Formation
Isugod Formation
Not Exposed
Discorbis sp.
Ammonia sp.
Elphidium sp.
Buccella sp.
Operculina sp.
Amphistegina sp.
Reef and forereef (<50 m), locally lagoon
Gyroidinoides soldanii
Pullenia bulloides
Uvigerina proboscidea
Bolivinita quadrilatera
Melonis pompilioides
Globocassidulina subglobosa
Middle bathyal (600–1000 m)
Amphistegina sp.
Elphidium sp.
Reef and forereef (<50 m)
Mudstone
Calcareous mudstone
Pebbly mudstone
Sandstone
Conglomerate
Limestone

Figure 6.

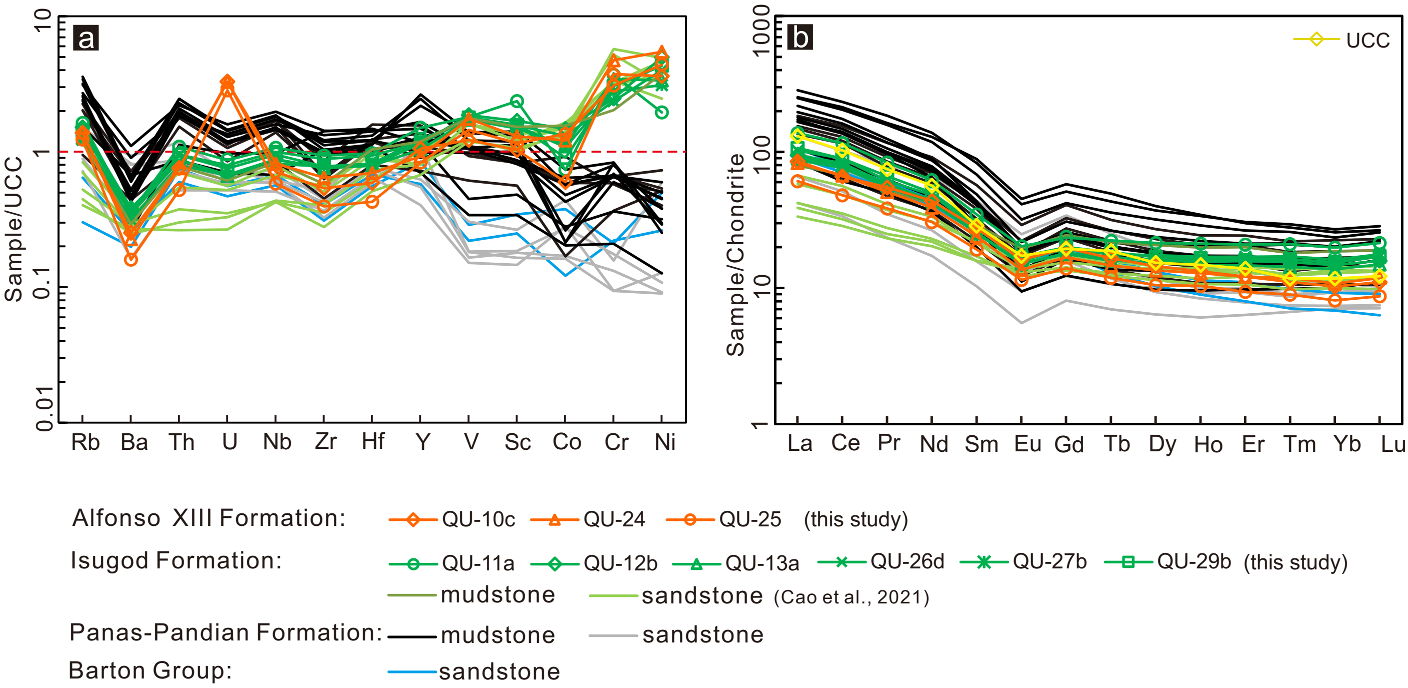
a
b
Sample/UCC
Sample/Chondrite
0.01
0.1
1
10
100
1000
Rb Ba Th U Nb Zr Hf Y V Sc Co Cr Ni
La Ce Pr Nd Sm Eu Gd Tb Dy Ho Er Tm Yb Lu
UCC
Alfonso XIII Formation: QU-10c QU-24 QU-25 (this study)
Isugod Formation: QU-11a QU-12b QU-13a QU-26d QU-27b QU-29b (this study)
mudstone sandstone (Cao et al., 2021)
Panas-Pandian Formation: mudstone sandstone
Barton Group: sandstone

Figure 7.

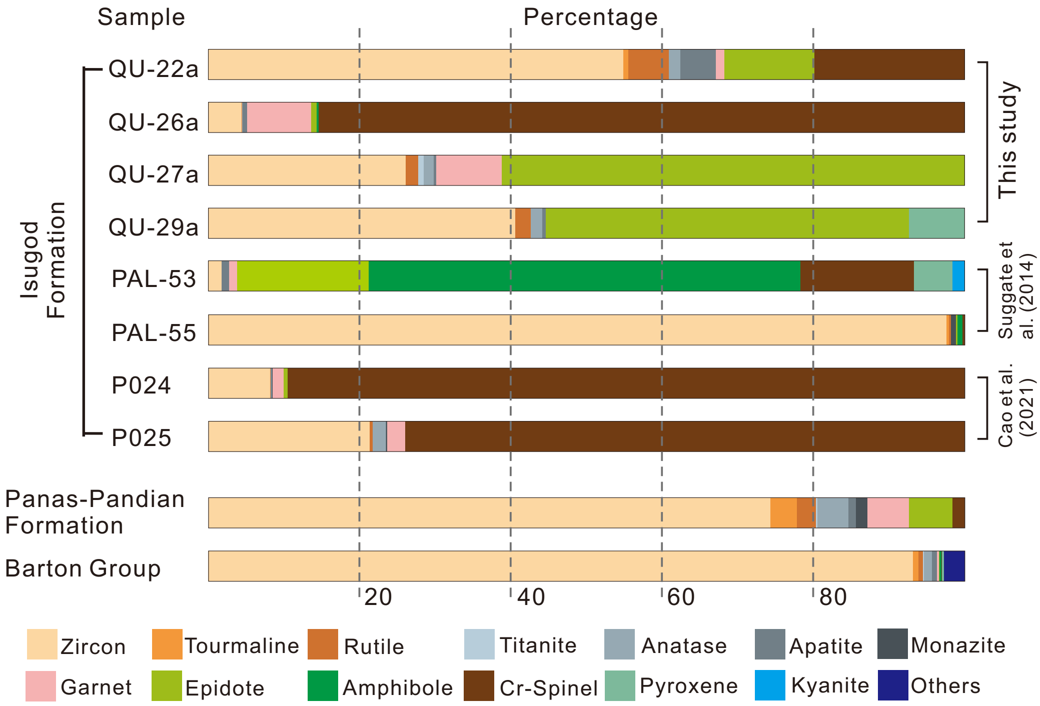

Sample
Percentage
QU-22a
QU-26a
QU-27a
QU-29a
PAL-53
PAL-55
P024
P025
Isugod Formation
This study
Suggate et al. (2014)
Cao et al. (2021)
Panas-Pandian Formation
Barton Group
20
40
60
80
Zircon
Tourmaline
Rutile
Titanite
Anatase
Apatite
Monazite
Garnet
Epidote
Amphibole
Cr-Spinel
Pyroxene
Kyanite
Others

Figure 8.

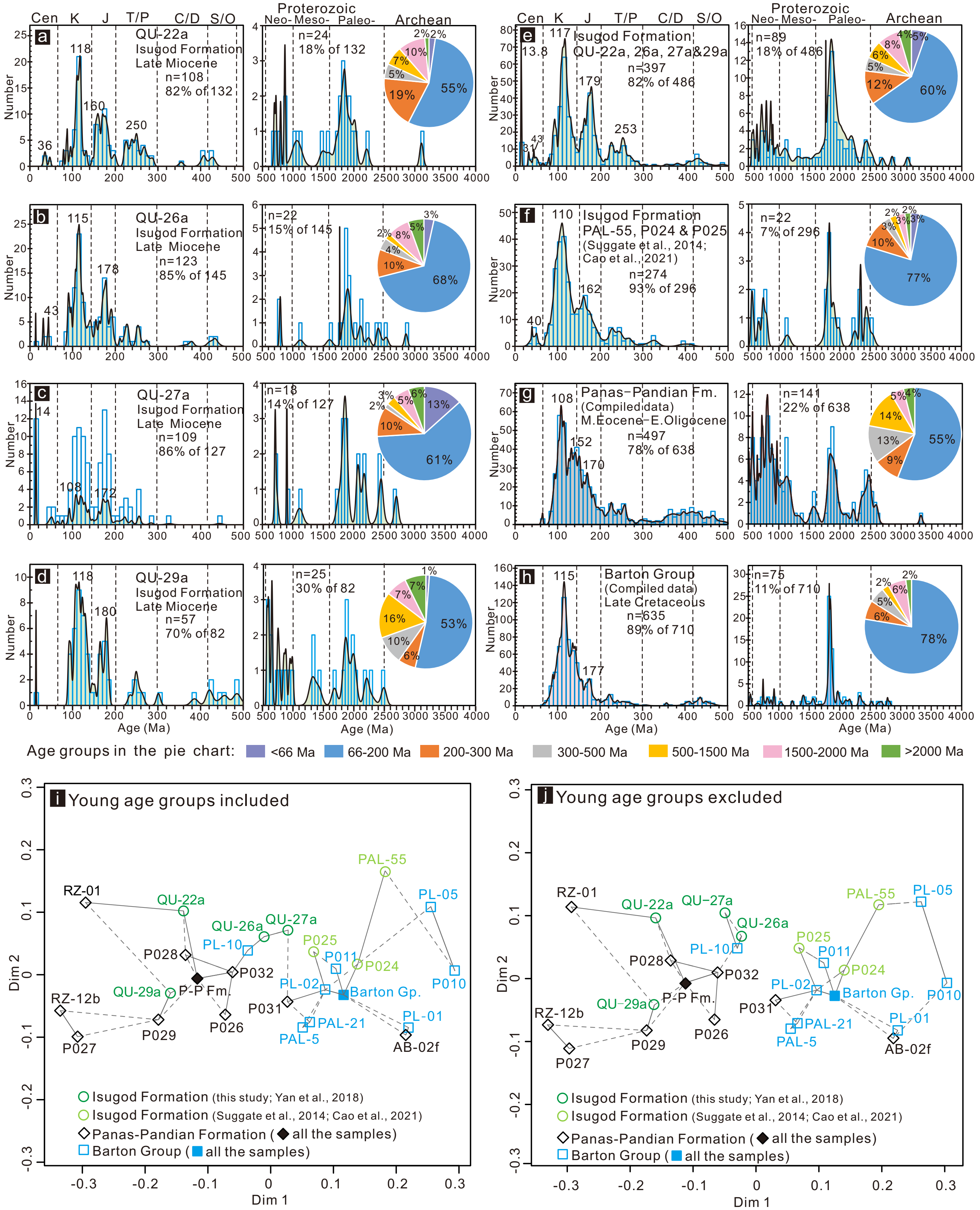

QU-22a
Isugod Formation
Late Miocene
QU-26a
QU-27a
QU-29a
Isugod Formation
QU-22a, 26a, 27a&29a
Isugod Formation
PAL-55, P024 & P025
(Suggate et al., 2014; Cao et al., 2021)
Panas–Pandian Fm.
(Compiled data)
M.Eocene–E.Oligocene
Barton Group
(Compiled data)
Late Cretaceous
Age (Ma)
Number
Age groups in the pie chart: <66 Ma 66-200 Ma 200-300 Ma 300-500 Ma 500-1500 Ma 1500-2000 Ma >2000 Ma
Young age groups included
Young age groups excluded
Dim 1
Dim 2
Isugod Formation (this study; Yan et al., 2018)
Isugod Formation (Suggate et al., 2014; Cao et al., 2021)
Panas-Pandian Formation (all the samples)
Barton Group (all the samples)

Figure 9.

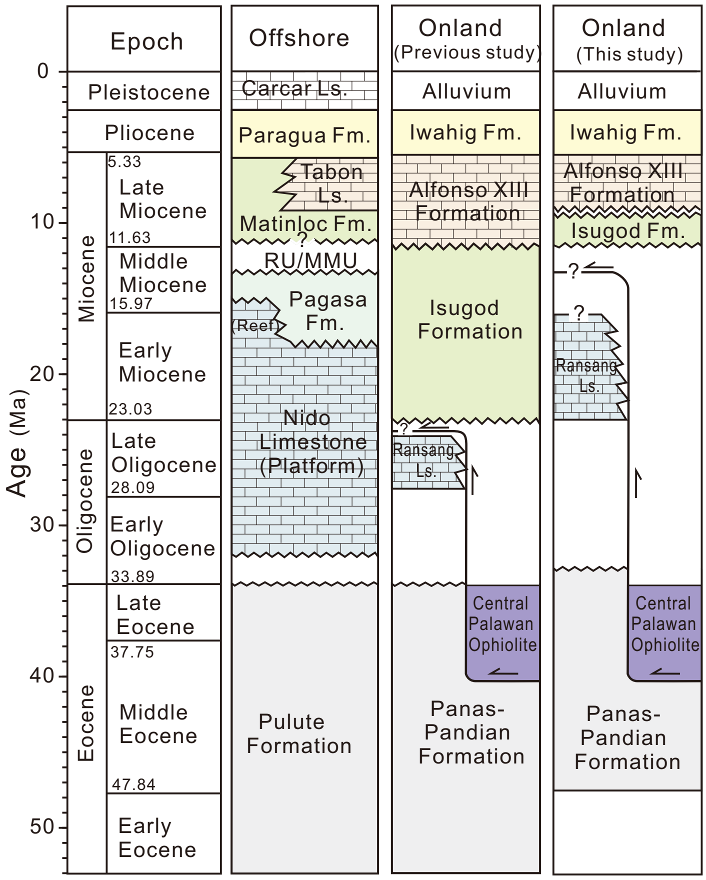

Epoch
Offshore
Onland
(Previous study)
Onland
(This study)
Age (Ma)
0
10
20
30
40
50
Pleistocene
Pliocene
Miocene
Late Miocene
Middle Miocene
Early Miocene
Oligocene
Late Oligocene
Early Oligocene
Eocene
Late Eocene
Middle Eocene
Early Eocene
5.33
11.63
15.97
23.03
28.09
33.89
37.75
47.84
Carcar Ls.
Paragua Fm.
Tabon Ls.
Matinloc Fm.
?
RU/MMU
Pagasa Fm.
(Reef)
Nido Limestone (Platform)
Pulute Formation
Alluvium
Iwahig Fm.
Alfonso XIII Formation
Isugod Formation
?
Ransang Ls.
Central Palawan Ophiolite
Panas-Pandian Formation
Alluvium
Iwahig Fm.
Alfonso XIII Formation
Isugod Fm.
?
?
Ransang Ls.
Central Palawan Ophiolite
Panas-Pandian Formation

Figure 10.

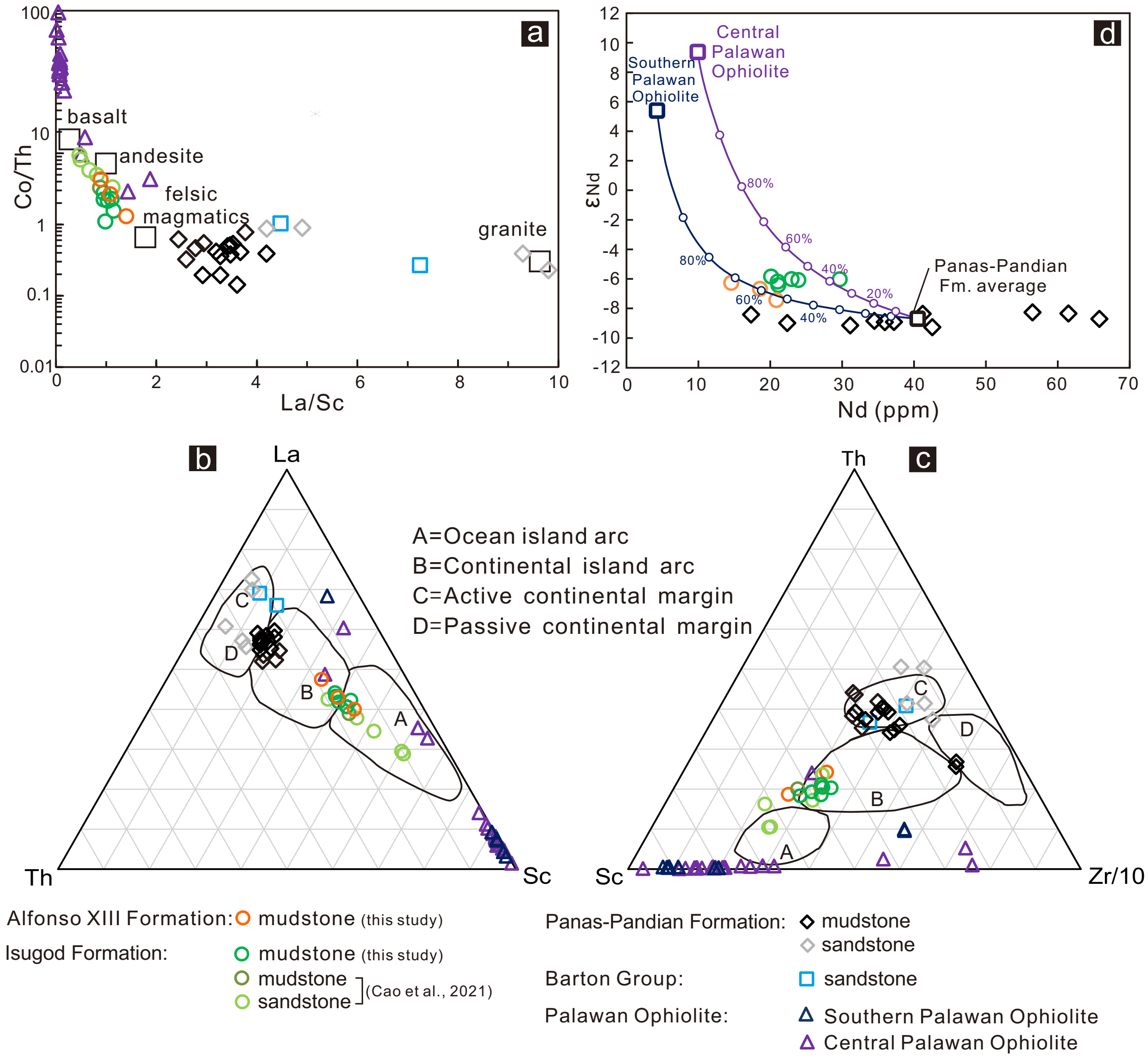

a
Co/Th
La/Sc
basalt
andesite
felsic
magmatics
granite
d
εNd
Nd (ppm)
Central
Palawan
Ophiolite
Southern
Palawan
Ophiolite
Panas-Pandian
Fm. average
80%
60%
40%
20%
b
La
Th
Sc
A=Ocean island arc
B=Continental island arc
C=Active continental margin
D=Passive continental margin
c
Th
Sc
Zr/10
Alfonso XIII Formation: mudstone (this study)
Isugod Formation: mudstone (this study)
mudstone
sandstone
(Cao et al., 2021)
Panas-Pandian Formation: mudstone
sandstone
Barton Group: sandstone
Palawan Ophiolite: Southern Palawan Ophiolite
Central Palawan Ophiolite

Figure 11.

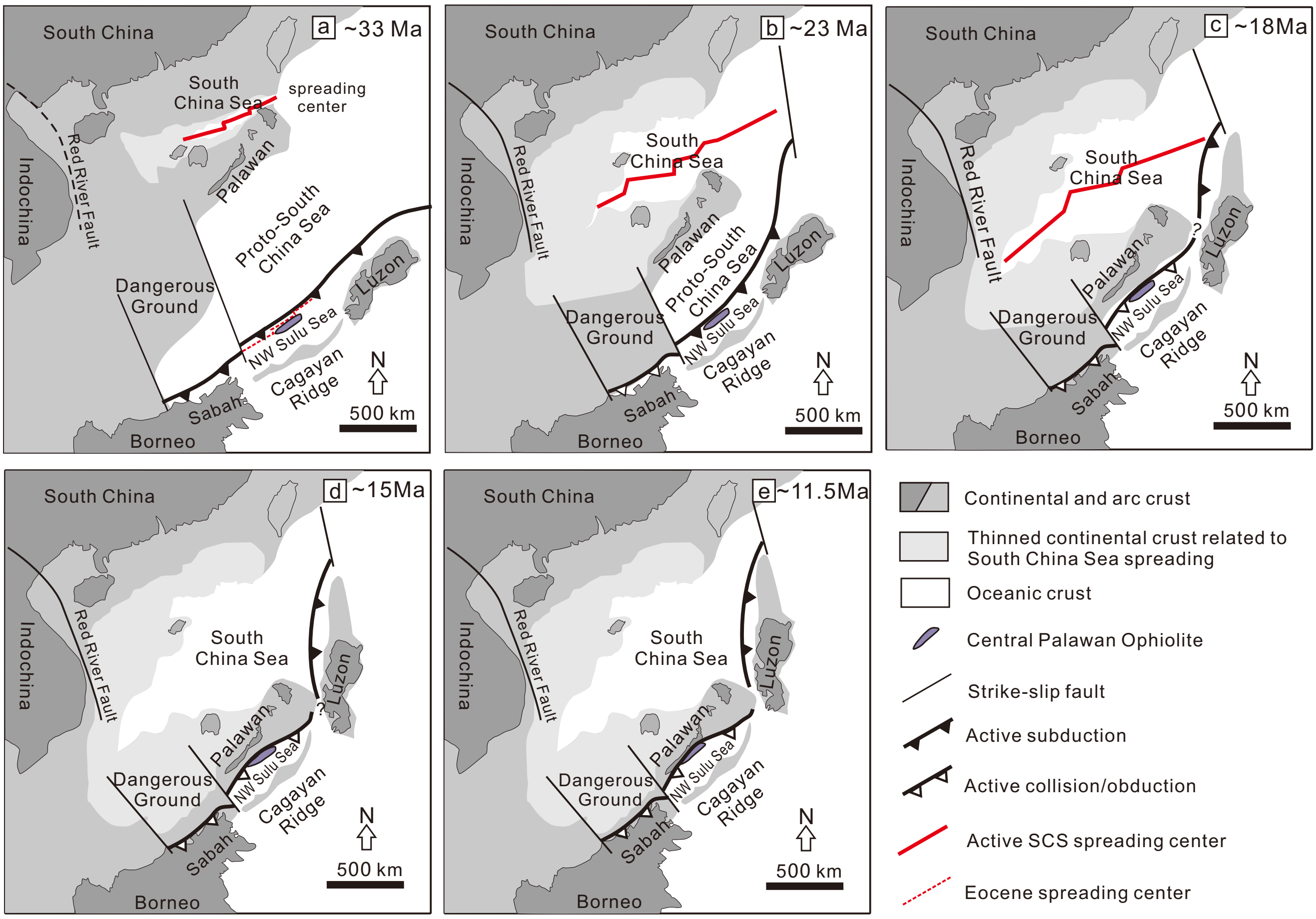

a ~33 Ma
South China
South China Sea
spreading center
Palawan
Proto-South China Sea
Indochina
Red River Fault
Dangerous Ground
NW Sulu Sea
Luzon
Cagayan Ridge
Sabah
Borneo
N
500 km
b ~23 Ma
c ~18Ma
d ~15Ma
e ~11.5Ma
Continental and arc crust
Thinned continental crust related to South China Sea spreading
Oceanic crust
Central Palawan Ophiolite
Strike-slip fault
Active subduction
Active collision/obduction
Active SCS spreading center
Eocene spreading center

Figure 12.

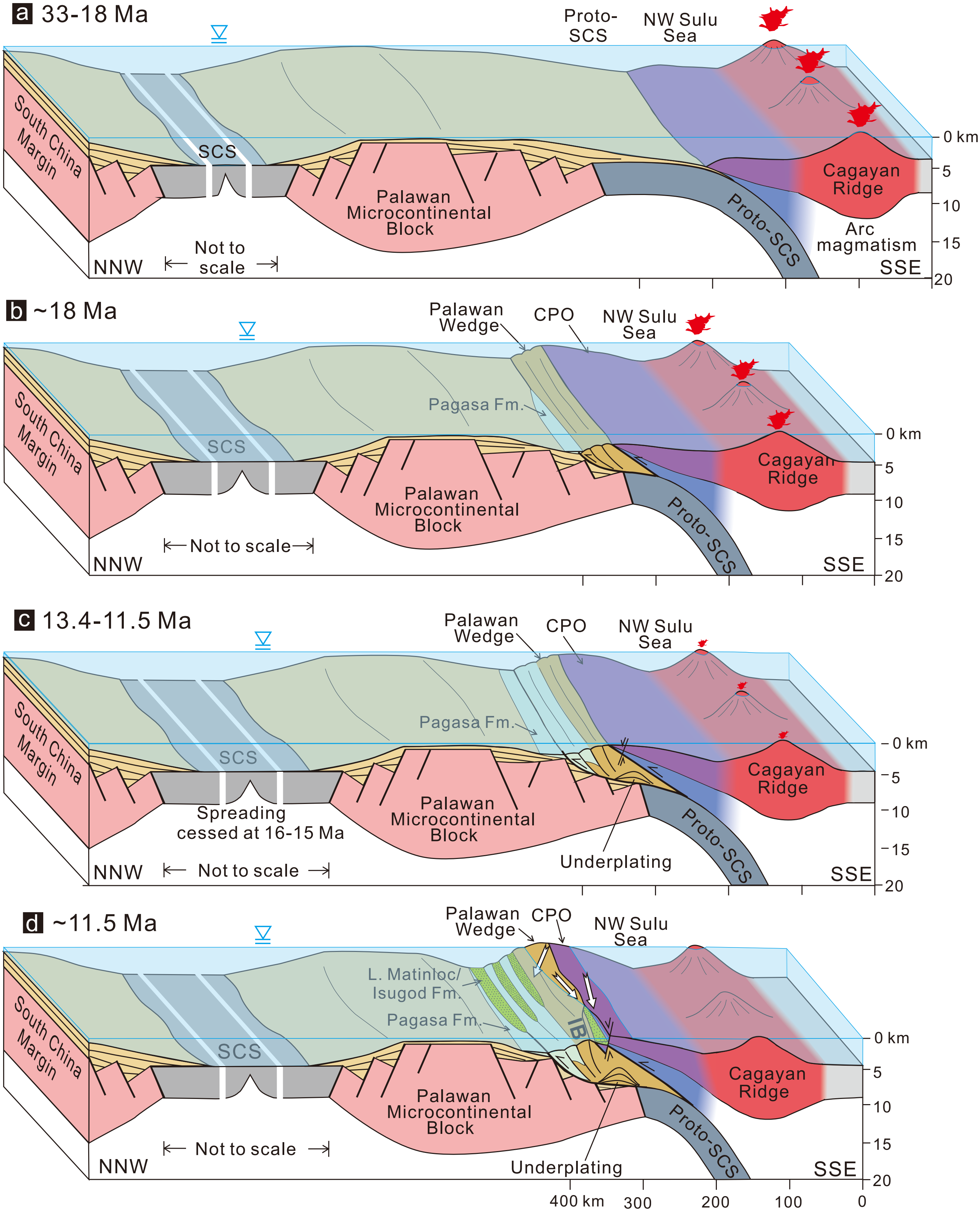

a 33-18 Ma
Proto-SCS
NW Sulu Sea
South China Margin
SCS
Palawan Microcontinental Block
Proto-SCS
Cagayan Ridge
Arc magmatism
Not to scale
NNW
SSE
0 km
5
10
15
20
b ~18 Ma
Palawan Wedge
CPO
NW Sulu Sea
Pagasa Fm.
South China Margin
SCS
Palawan Microcontinental Block
Proto-SCS
Cagayan Ridge
Not to scale
NNW
SSE
0 km
5
10
15
20
c 13.4-11.5 Ma
Palawan Wedge
CPO
NW Sulu Sea
Pagasa Fm.
South China Margin
SCS
Spreading cessed at 16-15 Ma
Palawan Microcontinental Block
Underplating
Proto-SCS
Cagayan Ridge
NNW
Not to scale
SSE
0 km
5
10
15
20
d ~11.5 Ma
Palawan Wedge
CPO
NW Sulu Sea
L. Matinloc/ Isugod Fm.
Pagasa Fm.
IB
South China Margin
SCS
Palawan Microcontinental Block
Underplating
Proto-SCS
Cagayan Ridge
Not to scale
NNW
SSE
0 km
5
10
15
20
400 km
300
200
100
0